

An Algorithm for Correct Computation of Reeb Spaces for PL Bivariate Fields

Amit Chattopadhyay ✉ 

International Institute of Information Technology, Bangalore 560100, India

Yashwanth Ramamurthi ✉ 

International Institute of Information Technology, Bangalore 560100, India

Osamu Saeki ✉ 

Institute of Mathematics for Industry, Kyushu University, Fukuoka 819-0395, Japan

Abstract

The Reeb space is a topological structure which is a generalization of the notion of the Reeb graph to multi-fields. Its effectiveness has been established in revealing topological features in data across diverse computational domains which cannot be identified using the Reeb graph or other scalar-topology-based methods. Approximations of Reeb spaces such as the Mapper and the Joint Contour Net have been developed based on quantization of the range. However, computing the topologically correct Reeb space dispensing the range-quantization is a challenging problem. In the current paper, we develop an algorithm for computing a correct net-like approximation corresponding to the Reeb space of a generic piecewise-linear (PL) bivariate field based on a multi-dimensional Reeb graph (MDRG). First, we prove that the Reeb space is homeomorphic to its MDRG. Subsequently, we introduce an algorithm for computing the MDRG of a generic PL bivariate field through the computation of its Jacobi set and Jacobi structure, a projection of the Jacobi set into the Reeb space. This marks the first algorithm for MDRG computation without requiring the quantization of bivariate fields. Following this, we compute a net-like structure embedded in the corresponding Reeb space using the MDRG and the Jacobi structure. We provide the proof of correctness and complexity analysis of our algorithm.

Keywords and phrases Reeb Space, Piecewise-Linear Bivariate Field, Multi-Dimensional Reeb Graph, Jacobi Set, Jacobi Structure, Algorithm.

Acknowledgements The authors would like to thank the Science and Engineering Research Board (SERB), India (SERB/CRG/2018/000702) and International Institute of Information Technology (IIITB), Bangalore for funding this project and for generous travel support.

1 Introduction

Multi-field topology has become increasingly prominent due to its richness compared to scalar topology. Techniques for computing multi-field topology have been developed based on Jacobi sets [9], fibers [20], and Reeb spaces [12]. Tools in multi-field topology have proven to be effective in revealing features which cannot be detected using scalar topology tools [8, 3, 18]. In particular, the Reeb space is a topological structure that extends the concept of the Reeb graph to multi-fields by generalizing the contour topology of a scalar field to encompass the fiber topology of a multi-field [12]. Its applications span diverse fields such as shape-matching [23], quantum chemistry [24], computational physics [1], and climate data analysis [15]. Range-based quantized approximations of the Reeb space such as the Mapper [23] and Joint Contour Net (JCN) [2] have been developed. Nevertheless, determining the appropriate levels of quantization to correctly represent the underlying topology of the data remains a challenge in these methods.

Furthermore, the problem of computing the Reeb space of generic piecewise-linear (PL) maps (or multi-fields) dispensing the quantization of the range is also challenging. Edelsbrunner et al. [12] sketched the theory behind developing an algorithm for computing

Reeb spaces of generic PL maps. However, no practical algorithm has been developed based on this theory until now. Tierny et al.[24] designed an algorithm to compute the Reeb space of a PL bivariate field dispensing the quantization by developing the notion of *Jacobi fiber surface*. However, this algorithm necessitates the computation of the Jacobi fiber surface passing through the edges of the PL *Jacobi set*. Taking a different approach, we devise an algorithm to compute a net-like structure corresponding to the Reeb space of a bivariate field based on its multi-dimensional Reeb graph (MDRG) [4]. Towards this, our contributions in the current paper are as follows:

- First, we show that the MDRG of a bivariate field is homeomorphic to its Reeb space. This result is crucial in the computation of Reeb space (Section 4).
- Then we present an algorithm for computing the MDRG of a PL bivariate field by computing its Jacobi structure (Section 5), which is the projection of the Jacobi set on the Reeb space. An algorithm for computing the Jacobi structure is discussed in Section 5.2.
- Finally, we present an algorithm for computing a net-like structure embedded in the corresponding Reeb space, using the MDRG and Jacobi structure. We provide the proof of correctness of our algorithm (Section 5.4).
- We also give the complexity analysis of our algorithm (Section 6).

Outline. Section 2 discusses the related works in the development of tools in multi-field topology. Section 3 offers the essential background for understanding the proposed algorithm. Section 4 provides a proof of homeomorphism between the Reeb space and the MDRG of a PL bivariate field. Section 5 outlines an algorithm for computing the MDRG corresponding to a PL bivariate field. Section 5.1 provides criteria for detecting points of topological changes on the first dimensional Reeb graph. Section 5.2 presents the algorithm for computing the Jacobi structure. In Section 5.3 we provide an algorithm for computing MDRG of a PL bivariate field. In Section 5.4, we discuss the algorithm for computing a net-like structure embedded in the Reeb space corresponding to a PL bivariate field and provide the proof of correctness of our algorithm. In Section 6, we analyze the complexity of the proposed algorithms for computing the Reeb space of a PL bivariate field. Finally, a conclusion is drawn in Section 7.

2 Previous Works

Recently, there has been a growing interest in the development of tools in multi-field topology, driven by their ability to capture features compared to scalar topology. Edelsbrunner et al.[9] demonstrate the applicability of Jacobi sets in studying protein interactions and Lagrange points in the solar system. Edelsbrunner et al.[12] introduced an algorithm for computing the Reeb space. However, no documentation of an implementation of this algorithm seems to have been reported [24]. Nevertheless, quantized approximations of the Reeb space have been developed. In particular, Singh et al.[23] introduced a mapper data structure for capturing the topology of high-dimensional point cloud data. Carr et al.[2] introduced the joint contour net (JCN) as a quantized approximation of the Reeb space, representing a specific case of the mapper. Duke et al.[8] demonstrated the usefulness of the JCN in visualizing nuclear scission in multi-field density functional theory (DFT) data.

Carr et al.[3] extended the concept of isosurfaces to bivariate fields by introducing *fiber surfaces*, and showcased their utility in datasets from chemistry, cosmology, and combustion. Distances between quantized Reeb spaces (JCNs) have been developed, and their applications have been demonstrated in computational physics [1], computational chemistry [18], and

shape matching [19]. Klotz et al.[15] developed an algorithm for computing the Jacobi set and demonstrated its effectiveness in fluid dynamics and climate datasets. Sharma et al.[22] recently introduced an output-sensitive algorithm for computing fiber surfaces for bivariate fields based on the Jacobi set.

A challenge in methods based on quantized Reeb spaces is the selection of appropriate quantization levels to capture the correct topology. Addressing this, Tierny et al.[24] formulated an algorithm for computing the Reeb space of a PL bivariate field without relying on the quantization of the range. However, this algorithm requires the computation of the fiber surface corresponding to each edge in the Jacobi set. In the current paper, we adopt a distinct approach by initially computing the MDRG and Jacobi structure of the bivariate field, which are subsequently used to compute a net-like structure corresponding to the Reeb space.

3 Background

In this section, we describe the necessary background in scalar and multi-field topology defined on a compact, orientable d -dimensional manifold \mathcal{M} without boundary. For the current paper, we need to consider $d = 3$ and $d = 2$. Since most of the data comes as a discrete set of real numbers at the grid points (vertices) of a mesh, we consider a simplicial complex approximation of \mathcal{M} .

3.1 Simplicial Complex

An i -simplex σ is the convex hull of a set S of $i + 1$ affinely independent points, and its dimension is i [10]. A *face* of σ is the convex hull of a non-empty subset of S . A *simplicial complex* K is a finite collection of simplices, where the faces of a simplex in K also belong to K , and the intersection of any two simplices in K is either empty or a face of both the simplices. For a simplex $\sigma \in K$, its *star* is denoted by $\text{St } \sigma$, and is defined as the set of simplices which contain σ as a face. The *closed star* of σ is obtained by adding all the faces of the simplices in $\text{St } \sigma$. The *link* of σ , denoted as $\text{Lk } \sigma$, is the set of simplices belonging to the *closed star* of σ that do not intersect σ . Let $|K|$ be the underlying space described by K . If there exists a homeomorphism $h : |K| \rightarrow \mathcal{M}$, then we say $\mathbb{M} = (|K|, h)$ is a triangulation or mesh of \mathcal{M} . Further, \mathbb{M} is a *combinatorial d -manifold* if the link of every i -simplex in \mathbb{M} triangulates a combinatorial $(d - i - 1)$ -sphere [12].

3.2 PL Scalar Field

Scalar data is usually presented as a discrete set of real values at the vertices or grid points of a mesh, say \mathbb{M} , corresponding to a triangulation of a compact d -manifold \mathcal{M} . The vertex set of \mathbb{M} is represented as $V(\mathbb{M}) = \{\mathbf{v}_0, \mathbf{v}_1, \dots, \mathbf{v}_{n_v-1}\}$, where n_v is the number of vertices in \mathbb{M} . The discrete scalar data can be mathematically represented by a function $\hat{f} : V(\mathbb{M}) \rightarrow \mathbb{R}$. From this discrete map \hat{f} , a piecewise-linear (PL) scalar field $f : \mathbb{M} \rightarrow \mathbb{R}$ can be obtained as follows. At the vertices of \mathbb{M} , f takes the values of \hat{f} , and the values in higher dimensional simplices are determined through linear interpolation. The PL scalar field f is said to be *generic* if no two adjacent vertices of \mathbb{M} have the same f -value.

3.2.1 PL Critical Point

Consider a generic PL scalar field $f : \mathbb{M} \rightarrow \mathbb{R}$. Then, if \mathbf{v} and \mathbf{v}' are the endpoints of an edge in \mathbb{M} , it follows that $f(\mathbf{v}) \neq f(\mathbf{v}')$. The *lower link* of a vertex \mathbf{v} , denoted by $\text{Lk}_- \mathbf{v}$, is the

collection of simplices in $\text{Lk } \mathbf{v}$ whose vertices have smaller f -values than $f(\mathbf{v})$. The *upper link* $\text{Lk}^+ \mathbf{v}$ is defined, similarly. To determine the type of vertices we compute the reduced Betti numbers of their lower links.

Following the usual convention, the i -th Betti number β_i is the rank of the i -th homology group in \mathbb{Z}_2 coefficients. The reduced Betti number, denoted by $\tilde{\beta}_i$, is obtained as follows. If $i \geq 1$, then $\tilde{\beta}_i = \beta_i$. For $i = 0$ or -1 , there are two possibilities. If the lower link is non-empty, then $\tilde{\beta}_0 = \beta_0 - 1$ and $\tilde{\beta}_{-1} = 0$. Otherwise, $\tilde{\beta}_0 = \beta_0 = 0$ and $\tilde{\beta}_{-1} = 1$. We note, the reduced Betti numbers $\tilde{\beta}_i$ are non-negative integers. If all reduced Betti numbers of the lower link corresponding to a vertex \mathbf{v} vanish, then \mathbf{v} is called a *PL regular vertex* of f . Otherwise, \mathbf{v} is a *PL critical point* (vertex), and the corresponding function value $f(\mathbf{v})$ is a *critical value*. Further, if the reduced Betti numbers of $\text{Lk}_- \mathbf{v}$ in all dimensions sum up to 1, then \mathbf{v} is called a *simple critical point*, otherwise, \mathbf{v} is called a *degenerate critical point*. The *index* of a simple critical point \mathbf{v} is i if the reduced Betti number is $\tilde{\beta}_{i-1} = 1$. A simple critical vertex of index 0 is called a minimum and a simple critical vertex of index d is called a maximum. Any other critical point of index i is called an i -saddle when i is an integer that varies from 1 to $d - 1$. In particular, for $d = 3$ the simple critical vertices of indices 0, 1, 2 and 3 are referred to as *minima*, *1-saddles*, *2-saddles*, and *maxima*, respectively. The *level set* of f corresponding to a level value $a \in \mathbb{R}$ is defined as the pre-image $f^{-1}(a)$, and each connected component of the level set is called a *contour*. A value $a \in \mathbb{R}$ is a *regular value* of f if its level set $f^{-1}(a)$ does not pass through a PL critical point. We note, the generic PL function f is said to be *PL Morse* if:

- I. every critical point of f on \mathbb{M} is simple, and
- II. no two critical vertices of f on \mathbb{M} have the same f -value.

Next, we discuss the Reeb graph that captures the level-set topology of a PL Morse function.

3.2.2 Reeb Graph

The Reeb graph of a PL Morse function $f : \mathbb{M} \rightarrow \mathbb{R}$, denoted by \mathcal{RG}_f , is the quotient space obtained by contracting each contour of f to a point. The associated quotient map is denoted by q_f . In particular, if \mathbb{M} is a triangulation corresponding to a simply connected domain, then \mathcal{RG}_f does not contain any loop and is called a *contour tree*. A Reeb graph consists of a set of nodes, and arcs connecting the nodes. A point in the Reeb graph is referred to as a *node* if the corresponding contour passes through a critical point of f . Other (regular) points of the Reeb graph lie on the arcs of the Reeb graph and each of these points corresponds to a contour of f not containing any critical point of f . The degree of a node is defined as the number of arcs incident on it. The number of such arcs joining adjacent nodes with lesser function values is called the down-degree of the node and the number of such arcs joining adjacent nodes with higher function values is called the up-degree of the node. Each node of \mathcal{RG}_f is one of the following types [10]:

- (i) *minimum* (down-degree: 0, up-degree: 1) - corresponding to a minimum of f where a contour takes birth,
- (ii) *maximum* (down-degree: 1, up-degree: 0) - corresponding to a maximum of f where a contour dies,
- (iii) *down-fork* (down-degree: 2, up-degree: 1) - corresponding to a 1-saddle of f which merges two contours of f into single contour,
- (iv) *up-fork* (down-degree: 1, up-degree: 2) - corresponding to a index $(d - 1)$ saddle of f which splits a contour of f into two contours, and

- (v) *degree-2 critical node* (up-degree: 1, down-degree: 1) - corresponding to other critical points of indices between 1 and $d - 1$ which correspond to a change in the genus and not in the number of contours.

A Reeb graph with degree-2 critical nodes is also known as an augmented Reeb graph. Since f is PL Morse, there is a one-to-one correspondence between critical points of f and nodes of augmented \mathcal{RG}_f . We denote the collection of nodes and arcs of an augmented \mathcal{RG}_f by $V(\mathcal{RG}_f)$ and $Arcs(\mathcal{RG}_f)$, respectively. The evolution of the level set topology of f , for increasing values of f , can be traced by its Reeb graph. In particular, for $d = 3$, a minimum node of \mathcal{RG}_f corresponds to a minimum point where a contour takes birth. Similarly, a maximum node corresponds to a maximum point where a contour dies. A down-fork corresponds to a 1-saddle where two contours merge into a single contour. Similarly, an up-fork corresponds to a 2-saddle where a contour splits into two contours. A degree-2 node indicates a change in the genus of the contour. The corresponding critical points are also known as genus-change critical points [5].

Computing Reeb graphs. Numerous algorithms for computing Reeb graphs are available in the literature. Here, we spotlight a few of them. Harvey et al.[14] presented a randomized algorithm to compute the Reeb graph of a PL Morse function f defined on a 2-dimensional simplicial complex K by collapsing the contours of f in random order. The expected time complexity of the algorithm is $\mathcal{O}(m \log m)$, where m is the number of simplices in K . Parsa et al.[17] introduced a method that involves sweeping the vertices in K (the input simplicial complex) with increasing values of f and monitoring the connected components of the level sets of f . The changes in level set correspond to the merge, split, creation, or removal of components in the Reeb graph. The time complexity of the algorithm is $\mathcal{O}(m \log m)$, where m is the number of simplices in the 2-skeleton of K . Doriasamy et al.[7] devised a Reeb graph computation algorithm by first partitioning the input domain into interval volumes, each having Reeb graphs without loops. Then, the contour trees corresponding to each of the subdivided volumes are constructed, and these are interconnected to obtain the Reeb graph. The algorithm has a time complexity of $\mathcal{O}(n_v \log(n_v) + sn_t)$, where n_v and n_t represent the number of vertices and triangles in the input triangle mesh, respectively, and s is the number of saddles.

In the current paper, we need to encode the genus-change critical points (degree-2 critical nodes) in the Reeb graph as they are essential for computing the correct multi-dimensional Reeb graph and the Reeb space (see Section 5 for more details). Therefore, we construct the augmented Reeb graph, by projecting these genus-change saddle points on \mathcal{RG}_f as discussed by Chiang et al.[5]. For the identification of genus-change saddle points, we test the criticality of each vertex in \mathbb{M} , and identify the saddle points which map to the interior of an arc in \mathcal{RG}_f by the quotient map q_f . The augmented Reeb graph is obtained by subdividing arcs of \mathcal{RG}_f based on the insertion of degree-2 nodes corresponding to these saddle points. We call this procedure of computing augmented Reeb graph as `CONSTRUCTAUGMENTEDREEBGRAPH`(\mathbb{M} , f) in Section 5.

3.3 PL Multi-Field

Analogous to the definition for PL scalar field, a PL multi-field $\mathbf{f} = (f_1, \dots, f_r) : \mathbb{M} \rightarrow \mathbb{R}^r$ (with $d \geq r \geq 1$) is defined at the vertices of \mathbb{M} and linearly interpolated within each simplex of \mathbb{M} . The preimage of the map \mathbf{f} associated with a value $\mathbf{c} \in \mathbb{R}^r$, denoted as $\mathbf{f}^{-1}(\mathbf{c})$, is known as a *fiber*, and each connected component of a fiber is referred to as a *fiber-component* [20, 21]. Specifically, in the case of a scalar field, these are called *level sets* and *contours*,

respectively (see Section 3.2.2 for more details). We assume that \mathbf{f} is a *generic PL mapping*: i.e., the image of every i -simplex σ of dimension at most r is an i -simplex. Specifically, for $r = 1$ and $r = 2$, \mathbf{f} is called a generic PL scalar and a generic PL bivariate field, respectively.

Next, we briefly introduce the Jacobi set which is the generalization of the notion of critical points for the multi-fields.

3.3.1 Jacobi Set

The *Jacobi set* is an extension of the notion of critical points for multi-fields [9]. Intuitively, the Jacobi set of the multi-field, comprising r functions, is the collection of critical points of one function restricted to the intersection of the level sets of the remaining $r - 1$ functions. For a generic PL multi-field $\mathbf{f} : \mathbb{M} \rightarrow \mathbb{R}^r$, its Jacobi set consists of $(r - 1)$ -simplices of \mathbb{M} which are critical. We briefly describe the determination of these critical simplices here and refer the readers to [12] for more details.

Let σ be an $(r - 1)$ -simplex of \mathbb{M} . Consider a unit vector \mathbf{u} in the $(r - 1)$ -sphere \mathbb{S}^{r-1} , and let $h_{\mathbf{u}} : \mathbb{M} \rightarrow \mathbb{R}$ be the PL function defined as $h_{\mathbf{u}}(\mathbf{x}) = \langle \mathbf{f}(\mathbf{x}), \mathbf{u} \rangle$, which is the height of the image of \mathbf{x} in the direction \mathbf{u} . If the value of $h_{\mathbf{u}}$ is constant on a simplex $\sigma \in \mathbb{M}$, using definitions for a vertex, σ is defined as regular or critical for $h_{\mathbf{u}}$ provided the corresponding image $h_{\mathbf{u}}(\sigma)$ is regular or critical. Furthermore, σ is a simple critical simplex if $h_{\mathbf{u}}(\sigma)$ is simple critical. Note that the lower (upper) link of σ consists of simplices in the link having $h_{\mathbf{u}}$ -values strictly less (greater) than the values at the vertices of σ . Using the genericity condition, the upper and lower links of $h_{\mathbf{u}}(\sigma)$ cover all vertices of $\text{Lk } \sigma$ [24]. Then by applying reduced homology of the lower link of $h_{\mathbf{u}}(\sigma)$, as discussed in 3.2.1, we determine whether the simplex σ is regular or critical for $h_{\mathbf{u}}$. Furthermore, it can be determined whether a critical simplex is simple critical or not.

If σ is a $(r - 1)$ -simplex, then precisely two unit vectors exist for which their height functions remain constant on σ . Specifically, these vectors are the unit normals \mathbf{u} and $-\mathbf{u}$ corresponding to the image of σ in \mathbb{R}^r . The lower link of σ for the height function $h_{\mathbf{u}}$ is its upper link for the other height function $h_{-\mathbf{u}}$. We note, σ has only a single chance to be critical, as it is critical for $h_{\mathbf{u}}$ if and only if it is critical for $h_{-\mathbf{u}}$. The *Jacobi set* of \mathbf{f} , denoted by $\mathbb{J}_{\mathbf{f}}$, consists of the set of critical $(r - 1)$ -simplices in \mathbb{M} , along with their faces. A point $\mathbf{x} \in \mathbb{M}$ is a *singular (critical) point* of \mathbf{f} if $\mathbf{x} \in \mathbb{J}_{\mathbf{f}}$ and $\mathbf{f}(\mathbf{x})$ is a *singular (critical) value*. Otherwise, \mathbf{x} is said to be a *regular point*. A point $\mathbf{y} \in \mathbb{R}^r$ is said to be a *regular value* if $\mathbf{f}^{-1}(\mathbf{y})$ does not contain a singular point.

A generic PL multi-field \mathbf{f} is said to be *simple* if every $(r - 1)$ -simplex of $\mathbb{J}_{\mathbf{f}}$ is simple critical. If \mathbf{f} is a simple PL multi-field, then for sufficiently small values of r , $\mathbb{J}_{\mathbf{f}}$ is a manifold [12, 13]. In this paper, we deal with simple PL bivariate fields and assume that the Jacobi set is a 1-manifold. The topology of a multi-field is captured by a Reeb space which we briefly describe next.

3.3.2 Reeb Space

For a generic PL multi-field $\mathbf{f} : \mathbb{M} \rightarrow \mathbb{R}^r$, and a point $\mathbf{c} \in \mathbb{R}^r$, the inverse image $\mathbf{f}^{-1}(\mathbf{c})$ is called a *fiber*, and each connected component of $\mathbf{f}^{-1}(\mathbf{c})$ is called a *fiber-component* [20, 21]. We note, a fiber-component of \mathbf{f} can be considered as an equivalence class determined by an equivalence relation \sim on \mathbb{M} . Here, two points $\mathbf{x}, \mathbf{y} \in \mathbb{M}$ are considered equivalent (or $\mathbf{x} \sim \mathbf{y}$) if and only if $\mathbf{f}(\mathbf{x}) = \mathbf{f}(\mathbf{y}) = \mathbf{c}$, and both \mathbf{x} and \mathbf{y} belong to the same fiber-component of $\mathbf{f}^{-1}(\mathbf{c})$. We note, the preimage of a singular value is termed as a *singular fiber*, while the preimage of a regular value is known as a *regular fiber*. A fiber-component is categorized as

a *singular fiber-component* if it traverses a singular point. Otherwise, it is referred to as a *regular fiber-component*. It should be noted that a singular fiber may include one or more regular fiber-components. The Reeb space of \mathbf{f} is the quotient space $\mathcal{RS}_{\mathbf{f}}$, determined by the quotient map $q_{\mathbf{f}} : \mathbb{M} \rightarrow \mathcal{RS}_{\mathbf{f}}$, which contracts each fiber-component in \mathbb{M} to a unique point in $\mathcal{RS}_{\mathbf{f}}$ [12]. The Stein factorization of \mathbf{f} is the representation of \mathbf{f} as the composition of $q_{\mathbf{f}}$ and the unique continuous map $\bar{\mathbf{f}} : \mathcal{RS}_{\mathbf{f}} \rightarrow \mathbb{R}^r$. The following commutative diagram depicts the relationship between the maps \mathbf{f} , $q_{\mathbf{f}}$ and $\bar{\mathbf{f}}$.

$$\begin{array}{ccc} \mathbb{M} & \xrightarrow{\mathbf{f}} & \mathbb{R}^r \\ & \searrow q_{\mathbf{f}} & \nearrow \bar{\mathbf{f}} \\ & \mathcal{RS}_{\mathbf{f}} & \end{array}$$

In particular, for a generic PL bivariate field, the Reeb space $\mathcal{RS}_{\mathbf{f}}$ consists of a collection of 2-manifolds that are connected in complicated ways [12]. In the current paper, we present an algorithm for computing a net-like structure corresponding to the Reeb space of a simple PL bivariate field.

Next, we describe a multi-dimensional Reeb graph data-structure which we use to compute the Reeb space.

3.3.3 Multi-Dimensional Reeb Graph

A Multi-Dimensional Reeb Graph (MDRG) is a hierarchical decomposition of the Reeb space into a collection of Reeb graphs [4]. For a Reeb space $\mathcal{RS}_{\mathbf{f}}$ of a generic PL bivariate field $\mathbf{f} = (f_1, f_2) : \mathbb{M} \rightarrow \mathbb{R}^2$, we consider the decomposition as follows. First, we consider the Reeb Graph \mathcal{RG}_{f_1} of f_1 , assuming f_1 is PL Morse. Again for each $p \in \mathcal{RG}_{f_1}$ assume the restricted field $\tilde{f}_2^p \equiv f_2|_{C_p} : C_p \rightarrow \mathbb{R}$, where $C_p := q_{f_1}^{-1}(p)$ is the contour corresponding to p , is PL Morse. Then consider the Reeb Graph corresponding to each of these restricted scalar fields \tilde{f}_2^p . These quotient spaces are shown by the following commutative diagrams:

$$\begin{array}{ccc} \mathbb{M} & \xrightarrow{f_1} & \mathbb{R} \\ & \searrow q_{f_1} & \nearrow \bar{f}_1 \\ & \mathcal{RG}_{f_1} & \end{array} \quad \begin{array}{ccc} C_p & \xrightarrow{\tilde{f}_2^p} & \mathbb{R} \\ & \searrow q_{\tilde{f}_2^p} & \nearrow \bar{\tilde{f}_2^p} \\ & \mathcal{RG}_{\tilde{f}_2^p} & \end{array}$$

The hierarchical decomposition of the Reeb Space $\mathcal{RS}_{\mathbf{f}}$ into the Reeb Graphs \mathcal{RG}_{f_1} and $\mathcal{RG}_{\tilde{f}_2^p}$ for each $p \in \mathcal{RG}_{f_1}$ is called the Multi-Dimensional Reeb Graph (MDRG) and is denoted by $\text{MDRG}_{\mathbf{f}}$ [4]. Thus the decomposition of the Reeb Space of $\mathbf{f} = (f_1, f_2)$ into a MDRG can be defined as:

$$\text{MDRG}_{\mathbf{f}} = \left\{ (p_1, p_2) : p_1 \in \mathcal{RG}_{f_1}, p_2 \in \mathcal{RG}_{\tilde{f}_2^{p_1}} \right\}. \quad (1)$$

Similarly, for a generic PL multi-field $\mathbf{f} = (f_1, f_2, \dots, f_r) : \mathbb{M} \rightarrow \mathbb{R}^r$ (with suitable PL Morse assumptions on f_1 and restrictions of other component functions) the definition can be generalized as:

$$\text{MDRG}_{\mathbf{f}} = \left\{ (p_1, p_2, \dots, p_r) : p_1 \in \mathcal{RG}_{f_1}, p_2 \in \mathcal{RG}_{\tilde{f}_2^{p_1}}, \dots, p_r \in \mathcal{RG}_{\tilde{f}_r^{p_{r-1}}} \right\}. \quad (2)$$

In this paper, we develop an algorithm for computing the MDRG (see Section 5.3) for a generic PL bivariate field. The MDRG is then utilized in constructing a net-like structure of the Reeb space (see Section 5.4).

Next, we provide a brief description of the Jacobi structure, which is the projection of Jacobi set to the Reeb space.

3.3.4 Jacobi Structure

The Jacobi structure of the Reeb space $\mathcal{RS}_{\mathbf{f}}$ of a generic PL multi-field $\mathbf{f} : \mathbb{M} \rightarrow \mathbb{R}^r$ is denoted by $\mathcal{J}_{\mathbf{f}}$, and is defined as the projection of $\mathbb{J}_{\mathbf{f}}$ to $\mathcal{RS}_{\mathbf{f}}$ by the quotient map $q_{\mathbf{f}}$ [4]. A point in $\mathcal{RS}_{\mathbf{f}}$ represents a singular fiber-component only if it belongs to $\mathcal{J}_{\mathbf{f}}$; otherwise, it represents a regular fiber-component. Therefore, $\mathcal{J}_{\mathbf{f}}$ partitions the Reeb space into regular and singular components [4], and thereby plays an important role in capturing the Reeb space topology. As described in [4], generically the Jacobi structure of a bivariate field \mathbf{f} consists of 0- and 1-dimensional components. We note, with suitable PL Morse assumptions on the component functions, each point of the Jacobi structure is guaranteed to appear as a critical node of the lowest level Reeb graphs of an MDRG [4]. In particular, for a generic PL bivariate field $\mathbf{f} = (f_1, f_2)$ (with suitable PL Morse assumptions on the component functions) for the Jacobi structure of \mathbf{f} is captured by the critical nodes of the second dimensional Reeb graphs $\mathcal{RG}_{\tilde{f}_2^p}$ for $p \in \mathcal{RG}_{f_1}$. In the current paper, we assume that the functions \tilde{f}_2^p are PL Morse except at a discrete set of points p on \mathcal{RG}_{f_1} . In section 5.1, we detect these points (where one of the PL Morse conditions is violated) by analyzing the Jacobi structure to track the topological changes in the second-dimensional Reeb graphs of the MDRG.

Next, we briefly outline the topological changes in a time-varying Reeb graph which is a special case of the MDRG.

3.4 Time-Varying Reeb Graph

Edelsbrunner et al.[11] studied the topological changes in a time-varying Reeb graph of a 1-parameter family $f : \mathbb{M} \times \mathbb{R} \rightarrow \mathbb{R}$ of scalar fields based on the Jacobi set of the corresponding bivariate field $(t, f(\mathbf{x}, t)) : \mathbb{M} \times \mathbb{R} \rightarrow \mathbb{R}^2$ where \mathbb{M} is a 3-manifold without boundary. The restriction of f to a level set of the first field is denoted by $f_t : \mathbb{M} \times \{t\} \rightarrow \{t\} \times \mathbb{R}$ and the corresponding time-varying Reeb graph is denoted as \mathcal{RG}_{f_t} . The nodes of \mathcal{RG}_{f_t} correspond to the critical points of f_t which trace out the segments of the Jacobi curve as t varies. The function f_t is assumed to be a Morse function except at a discrete set of values of t where one of the Morse conditions may be violated. The topological changes in \mathcal{RG}_{f_t} , when t varies, are classified into two categories: (i) birth-death of a node - this happens when the Morse condition I is violated in f_t and (ii) swapping of nodes in the Reeb graphs - this happens when the Morse condition II is violated in f_t . The birth-death points correspond to points where the Jacobi set and the level sets of the component scalar fields (of the bivariate field) have a common normal. The Jacobi set is decomposed into segments by disconnecting at the birth-death points. It is shown that the indices of critical points remain the same on a segment and the indices of two critical points created or destroyed at a birth-death point differ by one. This is stated as *index lemma*:

► **Lemma 1. Index Lemma [11]:** *If $f : \mathbb{M} \times \mathbb{R} \rightarrow \mathbb{R}$ is a 1-parameter family of Morse functions, then at a birth-death point, the indices of the two critical points which are created or destroyed differ by exactly one.*

We utilize these observations in constructing the MDRG of a generic PL bivariate field $\mathbf{f} = (f_1, f_2)$. Specifically, we compute the points in the Reeb graph of f_1 , where there is a change in the topology of the second-dimensional Reeb graphs. We observe that these points are associated with critical points of f_1 restricted to the Jacobi set, and the double points of \mathbf{f} corresponding to crossings in the Jacobi structure $\mathcal{J}_{\mathbf{f}}$ as stated in Lemma 6.

In the current paper, we introduce an algorithm for computing the Reeb space of a bivariate field based on the MDRG. This stems from the homeomorphism between the MDRG and the Reeb space, which we prove in the next section.

4 Homeomorphism between Reeb Space and MDRG

In this section, we prove that the MDRG corresponding to a bivariate field is homeomorphic to its Reeb space. Consider a continuous map $\mathbf{f} = (f_1, f_2) : \mathcal{M} \rightarrow \mathbb{R}^2$. Note, \mathcal{M} is a d -dimensional manifold and $d \geq 2$. (However, in the statements and proofs of this section, \mathcal{M} can be any topological space.) Let us define $\omega_i : \mathcal{R}\mathcal{S}_{\mathbf{f}} \rightarrow \mathcal{R}\mathcal{G}_{f_i}$, $i = 1, 2$, as follows. Take $p \in \mathcal{R}\mathcal{S}_{\mathbf{f}}$. Set $\mathbf{r} = \bar{\mathbf{f}}(p) \in \mathbb{R}^2$ and $\mathbf{r} = (r_1, r_2)$. The point p corresponds to a connected component of

$$\mathbf{f}^{-1}(\mathbf{r}) = f_1^{-1}(r_1) \cap f_2^{-1}(r_2).$$

This is a nonempty connected subset of $f_i^{-1}(r_i)$: therefore, it is contained in a unique connected component of $f_i^{-1}(r_i)$. This corresponds to a point in $\mathcal{R}\mathcal{G}_{f_i}$, which we define to be $\omega_i(p)$. By this description, we see easily that ω_i is well defined.

By definition, it is clear that $\omega_i \circ q_{\mathbf{f}} = q_{f_i}$. As $\mathcal{R}\mathcal{S}_{\mathbf{f}}$ and $\mathcal{R}\mathcal{G}_{f_i}$ are endowed with the quotient topologies, we see immediately that ω_i is continuous. Thus we have the following commutative diagram of continuous maps:

Note that pr_i projects the range of the map \mathbf{f} onto the range of f_i , for $i = 1, 2$. Next, we provide the proof of homeomorphism between $\mathcal{R}\mathcal{S}_{\mathbf{f}}$ and $\mathcal{M}\mathcal{D}\mathcal{R}\mathcal{G}_{\mathbf{f}}$.

► **Lemma 2.** *For $p_1 \in \mathcal{R}\mathcal{G}_{f_1}$, the space $\mathcal{R}\mathcal{G}_{\tilde{f}_2^{p_1}}$ can be identified with the subspace $\omega_1^{-1}(p_1)$ of $\mathcal{R}\mathcal{S}_{\mathbf{f}}$ in a canonical way.*

Proof. Recall that $\tilde{f}_2^{p_1} = f_2|_{q_{f_1}^{-1}(p_1)}$. Let us first observe that $\mathcal{R}\mathcal{G}_{\tilde{f}_2^{p_1}}$ can be regarded as a subspace of $\mathcal{R}\mathcal{S}_{\mathbf{f}}$. First, a point in $\mathcal{R}\mathcal{G}_{\tilde{f}_2^{p_1}}$ corresponds to a connected component of $(f_2|_{q_{f_1}^{-1}(p_1)})^{-1}(r_2) = q_{f_1}^{-1}(p_1) \cap f_2^{-1}(r_2)$ for some $r_2 \in \mathbb{R}$. This component coincides with a unique connected component of $\mathbf{f}^{-1}(r_1, r_2) = f_1^{-1}(r_1) \cap f_2^{-1}(r_2)$, where $r_1 = \bar{f}_1(p_1)$, since $q_{f_1}^{-1}(p_1)$ is a connected component of $f_1^{-1}(r_1)$. This corresponds to a unique point of $\mathcal{R}\mathcal{S}_{\mathbf{f}}$. Furthermore, the mapping $\varphi : \mathcal{R}\mathcal{G}_{\tilde{f}_2^{p_1}} \rightarrow \mathcal{R}\mathcal{S}_{\mathbf{f}}$ thus obtained is obviously injective, since a point in $\mathcal{R}\mathcal{G}_{\tilde{f}_2^{p_1}}$ and its associated point in $\mathcal{R}\mathcal{S}_{\mathbf{f}}$ both correspond to the same connected component of an \mathbf{f} -fiber. Furthermore, the identification is canonical in this sense. In the following, we canonically identify $\mathcal{R}\mathcal{G}_{\tilde{f}_2^{p_1}}$ with its image by φ as a set.

Then, by definition, we see that $\omega_1(x) = p_1$ for every $x \in \mathcal{R}\mathcal{G}_{\tilde{f}_2^{p_1}}$. Therefore, we have

$$\mathcal{R}\mathcal{G}_{\tilde{f}_2^{p_1}} \subset \omega_1^{-1}(p_1).$$

On the other hand, for a point $y \in \mathcal{RS}_{\mathbf{f}}$, suppose $\omega_1(y) = p_1$. Set $\bar{\mathbf{f}}(y) = (r_1, r_2) \in \mathbb{R}^2$. Then, y corresponds to a connected component of $\mathbf{f}^{-1}(r_1, r_2) = f_1^{-1}(r_1) \cap f_2^{-1}(r_2)$. As $\omega_1(y) = p_1$, this is a connected component of $q_{f_1}^{-1}(p_1) \cap f_2^{-1}(r_2)$. This can be regarded as a point of $\mathcal{RG}_{\tilde{f}_2^{p_1}}$. Thus, we have $\mathcal{RG}_{\tilde{f}_2^{p_1}} = \omega_1^{-1}(p_1)$ as sets.

Let us now prove that their topologies coincide. For this, we need to show that the canonical injection $\varphi : \mathcal{RG}_{\tilde{f}_2^{p_1}} \rightarrow \mathcal{RS}_{\mathbf{f}}$ is actually an embedding. Since $\varphi \circ q_{\tilde{f}_2^{p_1}} = q_{\mathbf{f}}|q_{f_1}^{-1}(p_1)$, we see that φ is continuous.

Let us take a closed subset C of $\mathcal{RG}_{\tilde{f}_2^{p_1}}$. By definition, $q_{\tilde{f}_2^{p_1}}^{-1}(C)$ is a closed subset of $q_{f_1}^{-1}(p_1)$. As $q_{f_1}^{-1}(p_1)$ is a closed subset of \mathcal{M} , this means that $q_{\tilde{f}_2^{p_1}}^{-1}(C)$ is a closed subset of \mathcal{M} . Note that $q_{\mathbf{f}}^{-1}(\varphi(C)) = q_{\tilde{f}_2^{p_1}}^{-1}(C)$. This implies that $\varphi(C)$ is a closed subset of $\mathcal{RS}_{\mathbf{f}}$. Thus, this is also a closed subset of the image of φ . Hence, φ is a closed map.

Consequently, φ is a homeomorphism onto its image, i.e. an embedding. This completes the proof. \blacktriangleleft

Then, by the definition of the multi-dimensional Reeb graph together with the above lemma, we have

$$\text{MDRG}_{\mathbf{f}} = \{(p_1, p_2) \mid p_1 \in \mathcal{RG}_{f_1}, p_2 \in \omega_1^{-1}(p_1)\}. \quad (3)$$

As $p_1 = \omega_1(p_2)$ for $p_2 \in \omega_1^{-1}(p_1)$, and p_2 sweeps out all the points of $\mathcal{RS}_{\mathbf{f}}$ as p_1 ranges over all the points of \mathcal{RG}_{f_1} , we see that this space coincides with

$$\Gamma = \{(\omega_1(p_2), p_2) \mid p_2 \in \mathcal{RS}_{\mathbf{f}}\} \subset \mathcal{RG}_{f_1} \times \mathcal{RS}_{\mathbf{f}},$$

which is endowed with the product topology.

► **Remark 3.** In fact, $\text{MDRG}_{\mathbf{f}}$ is topologized through the above identification with Γ .

Let us define the map $h : \mathcal{RS}_{\mathbf{f}} \rightarrow \Gamma$ by $h(p) = (\omega_1(p), p)$ for $p \in \mathcal{RS}_{\mathbf{f}}$. This is obviously continuous and bijective. Furthermore, the inverse map of h is given by the restriction to Γ of the projection $\mathcal{RG}_{f_1} \times \mathcal{RS}_{\mathbf{f}} \rightarrow \mathcal{RS}_{\mathbf{f}}$ to the second factor, and is therefore continuous. This implies that h is a homeomorphism.

Thus, we get the following proposition.

► **Proposition 4.** $\text{MDRG}_{\mathbf{f}} = \{(p_1, p_2) \mid p_1 \in \mathcal{RG}_{f_1}, p_2 \in \mathcal{RG}_{\tilde{f}_2^{p_1}}\}$ is homeomorphic to $\mathcal{RS}_{\mathbf{f}}$.

In this paper, based on the above homeomorphism proof between $\text{MDRG}_{\mathbf{f}}$ and $\mathcal{RS}_{\mathbf{f}}$, we compute a net-like structure corresponding the Reeb space by embedding the second-dimensional Reeb graphs of the MDRG into the Reeb space. The next section provides an algorithm for computing $\text{MDRG}_{\mathbf{f}}$ and $\mathcal{RS}_{\mathbf{f}}$.

5 Computing The Multi-Dimensional Reeb Graph and Reeb Space

Let $\mathbf{f} = (f_1, f_2) : \mathbb{M} \rightarrow \mathbb{R}^2$ be a generic PL bivariate field where \mathbb{M} be a triangulation of a compact 3-manifold \mathcal{M} without boundary. We assume the function \mathbf{f} satisfies the following two conditions:

- (i) $\mathbf{f} = (f_1, f_2)$ is a simple PL multi-field,
- (ii) f_1 is PL Morse and the functions \tilde{f}_2^p are PL Morse except at a discrete set of points p on \mathcal{RG}_{f_1} .

The outline of our algorithm for computing $\text{MDRG}_{\mathbf{f}}$ and the Reeb space $\mathcal{RS}_{\mathbf{f}}$ is as follows:

1. First, we build the augmented Reeb graph of the first field, i.e. \mathcal{RG}_{f_1} , using the procedure `CONSTRUCTAUGMENTEDREEBGRAPH`(\mathbb{M}, f_1) as discussed in Section 3.2.2. Note that corresponding to each point p on the arcs of \mathcal{RG}_{f_1} we get a second-dimensional Reeb graph $\mathcal{RG}_{\tilde{f}_2^p}$ which builds the $\text{MDRG}_{\mathbf{f}}$.
2. In the second step, we identify the discrete points p on \mathcal{RG}_{f_1} where the second-dimensional Reeb graph $\mathcal{RG}_{\tilde{f}_2^p}$ experiences a topological change. These include (i) the nodes of \mathcal{RG}_{f_1} corresponding to the critical points (including the genus change critical points) of f_1 and (ii) the points of \mathcal{RG}_{f_1} at which \tilde{f}_2^p violates one of the genericity conditions of Morse functions. Thus, we introduce a minimal set of points in \mathcal{RG}_{f_1} , denoted by P , such that if \mathcal{RG}_{f_1} is augmented based on the points in P , then each arc α of augmented Reeb graph \mathcal{RG}_{f_1} fulfills the following two conditions: (i) \tilde{f}_1 is monotonic along α , and (ii) for two distinct points $p_1, p_2 \in \alpha$, the Reeb graphs $\mathcal{RG}_{\tilde{f}_2^{p_1}}$ and $\mathcal{RG}_{\tilde{f}_2^{p_2}}$ are topologically equivalent. We denote the minimal set of arcs obtained by the augmentation of P as $\text{Arcs}(\mathcal{RG}_{f_1})$. The detailed procedure for determining the points in P is given in Section 5.1.
3. Finally, corresponding to each arc α in $\text{Arcs}(\mathcal{RG}_{f_1})$ we select a representative point p . We denote the set of representative points by P_R . For each point p in P_R , we compute the second dimensional augmented Reeb graph $\mathcal{RG}_{\tilde{f}_2^p}$, using the procedure `CONSTRUCTAUGMENTEDREEBGRAPH`($q_{f_1}^{-1}, \tilde{f}_2^p$). These Reeb graphs, along with \mathcal{RG}_{f_1} , effectively capture the topology of $\text{MDRG}_{\mathbf{f}}$. The nodes of $\mathcal{RG}_{\tilde{f}_2^p}$ correspond to the critical points of \tilde{f}_2^p , and as we vary p , they trace out the segments of the Jacobi structure in the Reeb space. Our algorithm uses this mechanism for identifying the nodes in different second-dimensional Reeb graphs to build a net-like structure corresponding to the Reeb space $\mathcal{RS}_{\mathbf{f}}$.

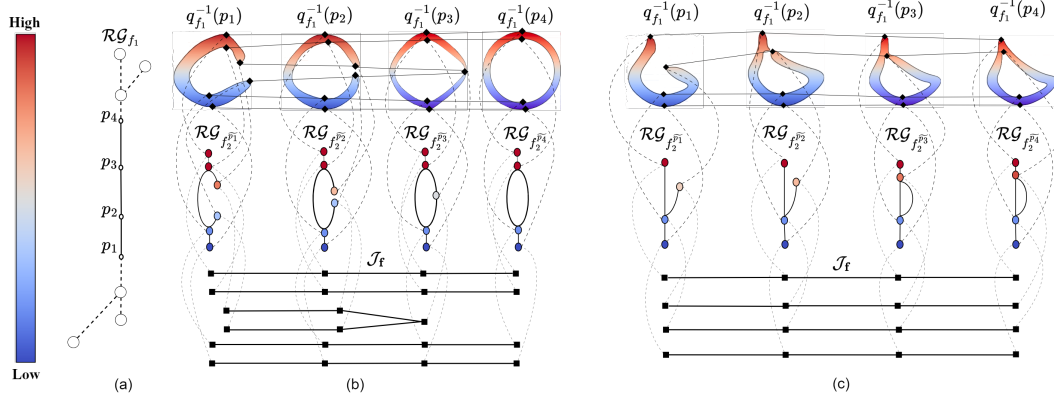
Next, we discuss steps 2 and 3 in more detail.

5.1 Detecting the Points of Topological Change on \mathcal{RG}_{f_1}

In this subsection, we provide the method for computing the set P , the set of points in \mathcal{RG}_{f_1} where the topology of $\mathcal{RG}_{\tilde{f}_2^p}$ changes as p varies in \mathcal{RG}_{f_1} . First, we provide the following definition for topological equivalence between two Reeb graphs $\mathcal{RG}_{\tilde{f}_2^{p_1}}$ and $\mathcal{RG}_{\tilde{f}_2^{p_2}}$ for $p_1, p_2 \in \mathcal{RG}_{f_1}$.

► **Definition 5.** *Two Reeb graphs $\mathcal{RG}_{\tilde{f}_2^{p_1}}$ and $\mathcal{RG}_{\tilde{f}_2^{p_2}}$ corresponding to two PL Morse functions $\tilde{f}_2^{p_1}$ and $\tilde{f}_2^{p_2}$ are topologically equivalent if the underlying functions $\tilde{f}_2^{p_1}$ and $\tilde{f}_2^{p_2}$ have the same sequence of critical points with similar index structures while traversing from the minimum to maximum values of the functions.*

We observe that the detection of a point $p \in \mathcal{RG}_{f_1}$ as a point of topological change is attributed to either by (i) a change in the topology of the domain on which the function \tilde{f}_2^p is defined, i.e. $q_{f_1}^{-1}(p)$ or by (ii) \tilde{f}_2^p violating one of the two genericity conditions of Morse function (in Section 3.2.1). The first case occurs when $q_{f_1}^{-1}(p)$ contains a critical point of f_1 , say \mathbf{x} . This critical point can induce the following topological changes in the contours of f_1 : (a) birth/death of a contour, (b) split or merge of contours, and (c) genus change of a contour. If \mathbf{x} belongs to the first two categories, then p will be either a minimum, a maximum, an up-fork, or a down-fork (as described in Section 3.2.2). In the third case of genus change, either a handle is added to $q_{f_1}^{-1}(p)$, or a handle is deleted from $q_{f_1}^{-1}(p)$. This results in a change in connectivity of the contours of \tilde{f}_2^p and, consequently, a change in the



1 **Figure 1** Topological changes in the second-dimensional Reeb graphs of the MDRG of a bivariate
 2 field $\mathbf{f} = (f_1, f_2)$ due to the critical points of f_1 . (a) Points along an arc of \mathcal{RG}_{f_1} . In both (b) and
 3 (c), the top row shows contours of f_1 colored based on the values of f_2 , critical points of f_2 restricted
 4 to the contours of f_1 , and the connectivity between the critical points based on the segments of the
 5 Jacobi set $\mathbb{J}_{\mathbf{f}}$. The middle row displays the corresponding second-dimensional Reeb graphs, while
 6 the Jacobi structure $\mathcal{J}_{\mathbf{f}}$ is presented in the bottom row. The contours of f_1 and the nodes of the
 7 Reeb graphs are colored based on the values of f_2 . Dotted lines illustrate the relationship between
 8 the critical points, Reeb graph nodes, and the points in $\mathcal{J}_{\mathbf{f}}$. In both the cases, a critical point of
 9 f_1 results in the addition of a handle in the contours of f_1 , leading to the formation of a loop in
 10 the second-dimensional Reeb graphs. Additionally, in (b), the loop-formation is also encoded by a
 11 maximum of f_1 restricted to $\mathbb{J}_{\mathbf{f}}$.

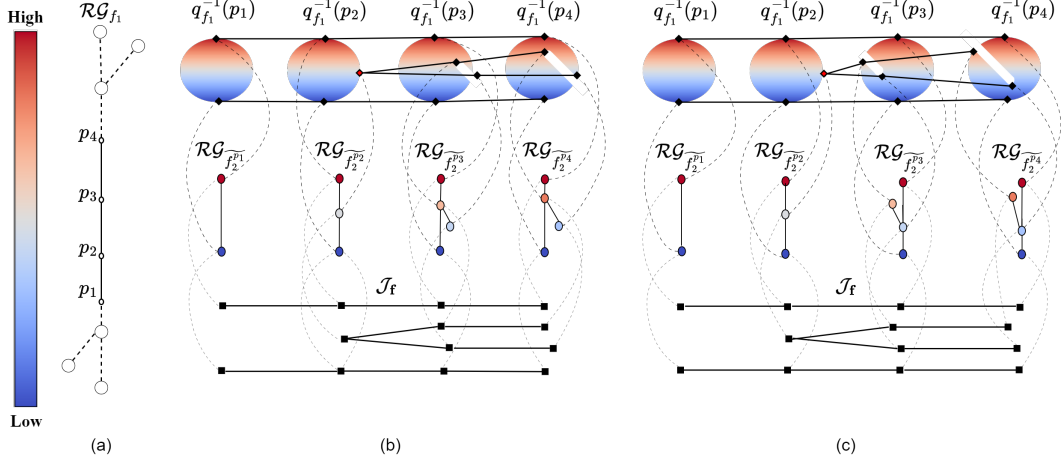
topology of $\mathcal{RG}_{\tilde{f}_2^p}$. In all three cases, p is detected as a node of the augmented Reeb graph \mathcal{RG}_{f_1} . Next, we discuss the topological changes arising from the violation of Morse criteria.

Generically, the function \tilde{f}_2^p is PL Morse. However, there are discrete points p on \mathcal{RG}_{f_1} at which \tilde{f}_2^p violates one of the genericity conditions of Morse functions. We detect topological changes in the second-dimensional Reeb graphs $\mathcal{RG}_{\tilde{f}_2^p}$ as point p varies on \mathcal{RG}_{f_1} , by examining the violation of one of the Morse criteria of the functions \tilde{f}_2^p . We note, the nodes of the second-dimensional Reeb graphs correspond to points in Jacobi structure $\mathcal{J}_{\mathbf{f}}$. As p varies along an arc of \mathcal{RG}_{f_1} , the nodes of $\mathcal{RG}_{\tilde{f}_2^p}$ are traced out by the $\mathcal{J}_{\mathbf{f}}$. Figures 1-3 show the relationship between the Reeb graph nodes with the points of the Jacobi structure and Jacobi set. Thus, we detect the points of topological change by examining $\mathbb{J}_{\mathbf{f}}$ and $\mathcal{J}_{\mathbf{f}}$. The following lemma characterizes the points of topological changes on \mathcal{RG}_{f_1} .

► **Lemma 6.** *The topology of $\mathcal{RG}_{\tilde{f}_2^p}$ changes at a point $p \in \mathcal{RG}_{f_1}$ if one of the following criteria is satisfied:*

- (C1) $q_{f_1}^{-1}(p)$ contains a critical point of f_1 .
- (C2) \tilde{f}_2^p violates the first Morse condition. Moreover, $q_{f_1}^{-1}(p)$ contains a critical point of f_1 restricted to the Jacobi set $\mathbb{J}_{\mathbf{f}}$.
- (C3) \tilde{f}_2^p violates the second Morse condition. In other words, there are two critical points of \tilde{f}_2^p belonging to the same contour of \tilde{f}_2^p . Alternatively, $q_{f_1}^{-1}(p)$ contains a point \mathbf{x} such that $q_{\mathbf{f}}(\mathbf{x})$ is a double point on the Jacobi structure $\mathcal{J}_{\mathbf{f}}$.

Proof. of (C1): Let $\mathbf{x} \in \mathbb{M}$ be a critical point of f_1 and $q_{f_1}(\mathbf{x}) = p$. Then p can indicate a change in the number of contours of f_1 , or a change in the genus of a contour [5]. If p

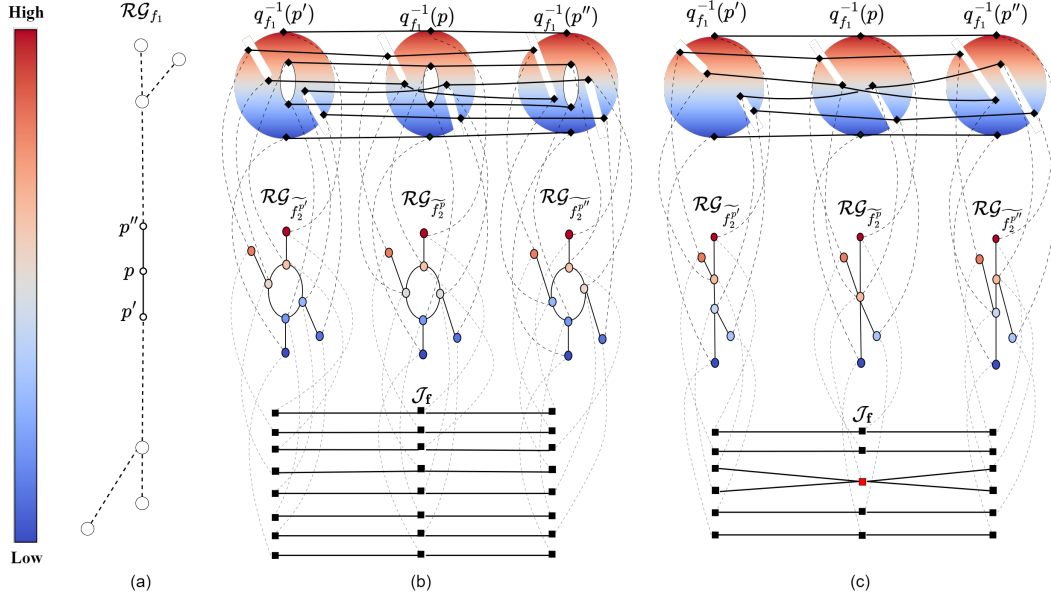


12 **Figure 2** Topological changes in the second-dimensional Reeb graphs of the MDRG for a bivariate
 13 field $\mathbf{f} = (f_1, f_2)$ due to the violation of the first Morse condition. (a) Points along an arc of \mathcal{RG}_{f_1} .
 14 (b) and (c) depict the birth of an arc in the second-dimensional Reeb graphs: (b) involving a
 15 minimum and down-fork, and (c) involving an up-fork and maximum. In both (b) and (c), the
 16 top row shows contours of f_1 colored based on the values of f_2 , critical points of f_2 restricted to
 17 the contours of f_1 , and the connectivity between the critical points based on the segments of the
 18 Jacobi set $\mathcal{J}_{\mathbf{f}}$. The middle row displays the corresponding second-dimensional Reeb graphs, while the
 19 Jacobi structure $\mathcal{J}_{\mathbf{f}}$ is presented in the bottom row. Dotted lines illustrate the relationship
 20 between the critical points, Reeb graphs nodes, and the points in $\mathcal{J}_{\mathbf{f}}$. In both the cases, the birth
 21 event is captured by a minimum of f_1 restricted to $\mathcal{J}_{\mathbf{f}}$.

belongs to the first category, then it is a minimum, a maximum, an up-fork, or a down-fork (as described in Section 3.2.2). Therefore, p is a node of \mathcal{RG}_{f_1} .

However, in the second case, the contour $q_{f_1}^{-1}(p)$ corresponds to a genus change. This event affects the topology of the domain on which \tilde{f}_2^p is defined, leading to a consequential change in the topology of $\mathcal{RG}_{\tilde{f}_2^p}$. Figure 1 illustrates two examples of this scenario. In both instances, the addition of a handle in the level set of f_1 results in the formation of a loop in the second-dimensional Reeb graph. We note, a change in the level set topology of f_1 by removal of a handle results in the deletion of a loop in the second-dimensional Reeb graph.

Proof of (C2): If \tilde{f}_2^p violates the first Morse condition, then \tilde{f}_2^p has a degenerate critical point, say \mathbf{x}_p . This corresponds to birth-death of a node in $\mathcal{RG}_{\tilde{f}_2^p}$ similar as discussed in Section 3.4. Let, $N(p)$ be a neighborhood of p in \mathcal{RG}_{f_1} so that the deleted neighborhood $N'(p)$ does not contain any node of \mathcal{RG}_{f_1} or any point t where \tilde{f}_2^t violates one of the Morse conditions. Let $p', p'' \in N(p)$ such that $f_1(p') < f_1(p) < f_1(p'')$. In the case of a birth event, $\tilde{f}_2^{p''}$ has a pair of critical points that are not present in $\tilde{f}_2^{p'}$. Further, each of the two critical points of $\tilde{f}_2^{p''}$ correspond to a node in $\mathcal{RG}_{\tilde{f}_2^{p''}}$, and these nodes are connected by an arc. Hence, a birth event signifies the birth of an arc in the second-dimensional Reeb graphs. According to the Index Lemma (see Lemma 1 of the present paper), the indices of two critical points created or destroyed at a birth-death point differ by an index of 1. Since the function $\tilde{f}_2^{p''}$ is defined on $q_{f_1}^{-1}(p'')$, which is a 2-manifold, critical points of $\tilde{f}_2^{p''}$ can have indices 0, 1, or 2. So there are two possibilities of indices: 0 – 1 or 1 – 2. If the two critical points have indices 0 and 1, then an arc connecting a minimum and a down-fork is born, as illustrated in Figure 2(b). Otherwise, if the indices are 1 and 2, then an arc connecting a maximum and



22 **Figure 3** Topological change in the second-dimensional Reeb graphs of the MDRG corresponding
 23 to a bivariate field $\mathbf{f} = (f_1, f_2)$ due to the violation of the second Morse condition. (a) Points p, p', p''
 24 along an arc of \mathcal{RG}_{f_1} . (b) and (c) depict two configurations of the second-dimensional Reeb graphs.
 25 In (b), two critical points of \tilde{f}_2^p share the same critical value but belong to different contours. In (c),
 26 two critical points of \tilde{f}_2^p are part of the same contour. In both (b) and (c), the top row shows the
 27 contours of f_1 colored based on the values of f_2 , critical points of f_2 restricted to the contours, and
 28 the connectivity between these critical points based on segments of the Jacobi set \mathcal{J}_f . The middle
 29 row displays the corresponding second-dimensional Reeb graphs, while the bottom row shows the
 30 Jacobi structure \mathcal{J}_f . In (c), the Reeb graph undergoes a topological change, which is captured by a
 31 self-intersection point of \mathcal{J}_f (shown in red).

an up-fork is born, as depicted in Figure 2(c).

The point \mathbf{x}_p corresponds to a birth-death point of the Jacobi set \mathcal{J}_f (see section 3.4). Specifically, two segments of \mathcal{J}_f diverge from or converge to \mathbf{x}_p referred to as birth or death events, respectively. As discussed in section 3.4, at the birth-death point \mathbf{x}_p the Jacobi set and the level sets of f_1 and f_2 have a common normal. In other words, locally, f_1 (similarly, f_2) is monotonic increasing along each of the Jacobi set segments meeting at \mathbf{x}_p . In the case of a birth event, \mathbf{x}_p is a minimum of f_1 restricted to \mathcal{J}_f , and in the case of a death event, it is a maximum. Thus a birth-death point is a critical point of f_1 restricted to the Jacobi set \mathcal{J}_f .

Proof of (C3): If \tilde{f}_2^p does not satisfy the second Morse condition, then \tilde{f}_2^p has two critical points \mathbf{x}_p and \mathbf{y}_p such that $\tilde{f}_2^p(\mathbf{x}_p) = \tilde{f}_2^p(\mathbf{y}_p)$. Let, $N(p)$ be a neighborhood of p on \mathcal{RG}_{f_1} which does not contain any critical node of \mathcal{RG}_{f_1} or any point t (other than p) such that \tilde{f}_2^p violates one of the genericity conditions. Consider $p', p'' \in N(p)$ such that $\tilde{f}_1(p') < \tilde{f}_1(p) < \tilde{f}_1(p'')$. Then, $\tilde{f}_2^{p'}$ and $\tilde{f}_2^{p''}$ are PL Morse functions. Let $\mathbf{x}_{p'}$ and $\mathbf{y}_{p'}$ be the critical points of $\tilde{f}_2^{p'}$ traced from \mathbf{x}_p and \mathbf{y}_p , respectively, each along a segment of \mathcal{J}_f . Similarly, let $\mathbf{x}_{p''}$ and $\mathbf{y}_{p''}$ be the critical points of $\tilde{f}_2^{p''}$ traced from \mathbf{x}_p and \mathbf{y}_p , respectively.

Since $\mathbf{x}_{p'}$ and $\mathbf{y}_{p'}$ are critical points of the PL Morse function $\tilde{f}_2^{p'}$, it follows that $f_2(\mathbf{x}_{p'}) \neq f_2(\mathbf{y}_{p'})$. Thus, $\mathbf{x}_{p'}$ and $\mathbf{y}_{p'}$ lie on different contours of $\tilde{f}_2^{p'}$, and therefore, $q_{\tilde{f}_2^{p'}}(\mathbf{x}_{p'})$ and $q_{\tilde{f}_2^{p'}}(\mathbf{y}_{p'})$ are two different nodes of the Reeb graph $\mathcal{RG}_{\tilde{f}_2^{p'}}$. Similarly, we have $f_2(\mathbf{x}_{p''}) \neq f_2(\mathbf{y}_{p''})$, and

$q_{\tilde{f}_2^{p''}}(\mathbf{x}_{p''}) \neq q_{\tilde{f}_2^{p''}}(\mathbf{y}_{p''})$. However, to identify whether p is a point of topological change, we need to check whether or not \mathbf{x}_p and \mathbf{y}_p belong to the same contour of \tilde{f}_2^p .

If \mathbf{x}_p and \mathbf{y}_p belong to the same contour of \tilde{f}_2^p , then they correspond to the same node of the Reeb graph $\mathcal{RG}_{\tilde{f}_2^p}$, i.e. $q_{\tilde{f}_2^p}(\mathbf{x}_p) = q_{\tilde{f}_2^p}(\mathbf{y}_p)$. Thus, the nodes $q_{\tilde{f}_2^{p'}}(\mathbf{x}_{p'})$ and $q_{\tilde{f}_2^{p'}}(\mathbf{y}_{p'})$ of $\mathcal{RG}_{\tilde{f}_2^{p'}}$ merge into a single node $q_{\tilde{f}_2^p}(\mathbf{x}_p) = q_{\tilde{f}_2^p}(\mathbf{y}_p)$ of $\mathcal{RG}_{\tilde{f}_2^p}$, which later splits into two nodes $q_{\tilde{f}_2^{p''}}(\mathbf{x}_{p''})$ and $q_{\tilde{f}_2^{p''}}(\mathbf{y}_{p''})$ of $\mathcal{RG}_{\tilde{f}_2^{p''}}$. Thus, p is a point of topological change in the second-dimensional Reeb graphs. Further, since each node in a second-dimensional Reeb graph of $\text{MDRG}_{\mathbf{f}}$ corresponds to a singular fiber component, this event signifies two singular fiber components merging into a single singular fiber component and later splitting into two singular fiber components. The Jacobi structure $\mathcal{J}_{\mathbf{f}}$, which captures the connectivity of singular fiber components, encodes this event as a self-intersection or double point. Figure 3(c) shows an illustration of this case.

However, if \mathbf{x}_p and \mathbf{y}_p belong to different contours of \tilde{f}_2^p , then they correspond to different nodes of $\mathcal{RG}_{\tilde{f}_2^p}$, i.e. $q_{\tilde{f}_2^p}(\mathbf{x}_p) \neq q_{\tilde{f}_2^p}(\mathbf{y}_p)$. Thus, even though \mathbf{x}_p and \mathbf{y}_p share the same f_2 -value, they do not induce merge/split of the contours of \tilde{f}_2^t for $t \in N(p)$. As a result, there is no change in the topology of the second-dimensional Reeb graphs. Figure 3(b) illustrates an example of this scenario. \blacktriangleleft

We note, under the genericity assumptions on \mathbf{f} , one of the conditions in Lemma 6 is also necessary for the topological change of $\mathcal{RG}_{\tilde{f}_2^p}$ at a point $p \in \mathcal{RG}_{f_1}$. From Lemma 6, it is evident that determining the points of topological change requires the following computations: (i) critical points of f_1 associated with genus changes, (ii) critical points of f_1 restricted to $\mathbb{J}_{\mathbf{f}}$, and (iii) double points of \mathbf{f} restricted to $\mathcal{J}_{\mathbf{f}}$. The first two requirements are fulfilled by examining the criticality of the vertices of \mathbb{M} and the vertices of the $\mathbb{J}_{\mathbf{f}}$. However, to fulfill the third requirement, we need to compute the Jacobi structure. Next, we discuss the algorithm for computing the Jacobi structure.

5.2 Algorithm: Computing Jacobi Structure

Consider a PL bivariate field $\mathbf{f} = (f_1, f_2)$ satisfying conditions (i) and (ii) in Section 5. The Jacobi set $\mathbb{J}_{\mathbf{f}}$ of \mathbf{f} is first computed as described in Section 3.3.1. In this subsection, we describe the computation of the Jacobi structure $\mathcal{J}_{\mathbf{f}}$, which is obtained as the projection of the Jacobi set $\mathbb{J}_{\mathbf{f}}$ into the Reeb space $\mathcal{RS}_{\mathbf{f}}$. Each point in $\mathcal{J}_{\mathbf{f}}$ represents a singular fiber-component of \mathbf{f} . Thus, $\mathcal{J}_{\mathbf{f}}$ is vital in determining the topology of $\mathcal{RS}_{\mathbf{f}}$. To compute the Jacobi structure $\mathcal{J}_{\mathbf{f}}$, we leverage the observation that the functions f_1 and f_2 are monotonic along the edges of $\mathbb{J}_{\mathbf{f}}$. This is followed by the genericity conditions of f_1 and f_2 .

Generically, $\mathbb{J}_{\mathbf{f}}$ is a PL 1-manifold [9]. However, the restriction of $q_{\mathbf{f}}$ to a component of $\mathbb{J}_{\mathbf{f}}$ may have a crossing, so the image may not be a 1-manifold (as shown in Figure 3(b)). The procedure for computing $\mathcal{J}_{\mathbf{f}}$ is outlined in Algorithm 1. For each edge $e(\mathbf{u}, \mathbf{v})$ of $\mathbb{J}_{\mathbf{f}}$, an edge $q_{\mathbf{f}}(e(\mathbf{u}, \mathbf{v}))$ is added to $\mathcal{J}_{\mathbf{f}}$ (lines 3-16, Algorithm 1). However, $q_{\mathbf{f}}(e(\mathbf{u}, \mathbf{v}))$ may intersect with a previously added edge $q_{\mathbf{f}}(e(\mathbf{u}', \mathbf{v}'))$ in $\mathcal{J}_{\mathbf{f}}$, as illustrated in Figure 4. Such an intersection occurs when $e(\mathbf{u}, \mathbf{v})$ and $e(\mathbf{u}', \mathbf{v}')$ intersect the same fiber-component of \mathbf{f} . As shown in Figure 4(d), the points $\mathbf{x} \in e(\mathbf{u}, \mathbf{v})$ and $\mathbf{y} \in e(\mathbf{u}', \mathbf{v}')$ lie on the same fiber-component. Thus $q_{\mathbf{f}}(e(\mathbf{u}, \mathbf{v}))$ and $q_{\mathbf{f}}(e(\mathbf{u}', \mathbf{v}'))$ intersect at $q_{\mathbf{f}}(\mathbf{x}) = q_{\mathbf{f}}(\mathbf{y})$. However, the determination of such intersections requires the computation of the augmented Reeb graph \mathcal{RG}_{f_1} which is performed by the procedure `CONSTRUCTAUGMENTEDREEBGRAPH` (line 17, Algorithm 1). The procedure `INTERSECTION` (called in line 20, Algorithm 1) computes such intersection points, which we detail next.

Algorithm 1 COMPUTEJACOBISTRUCTURE

Input: \mathbb{J}_f **Output:** \mathcal{J}_f

```

1: Initialize:  $\mathcal{J}_f = \emptyset$ 
2: for each edge  $e(\mathbf{u}, \mathbf{v})$  in  $\mathbb{J}_f$  do
3:   %Compute vertices for  $q_f(e(\mathbf{u}, \mathbf{v}))$ 
4:   if  $q_f(\mathbf{u})$  is not defined then
5:     Add a vertex  $u$  in  $\mathcal{J}_f$ 
6:     Set  $q_f(\mathbf{u}) = u$  and  $\tilde{\mathbf{f}}(u) = \mathbf{f}(\mathbf{u})$ 
7:   else
8:      $u = q_f(\mathbf{u})$ 
9:   end if
10:  if  $q_f(\mathbf{v})$  is not defined then
11:    Add a vertex  $v$  in  $\mathcal{J}_f$ 
12:    Set  $q_f(\mathbf{v}) = v$  and  $\tilde{\mathbf{f}}(v) = \mathbf{f}(\mathbf{v})$ 
13:  else
14:     $v = q_f(\mathbf{v})$ 
15:  end if
16:  Add the edge  $e(u, v)$  in  $\mathcal{J}_f$ 
17:   $\mathcal{RG}_{f_1} = \text{CONSTRUCTAUGMENTEDREEBGRAPH}(\mathbb{M}, f_1)$ 
18:  for each previously processed edge  $e(\mathbf{u}', \mathbf{v}')$  of  $\mathbb{J}_f$  do
19:    %Compute the intersection of  $q_f(e(\mathbf{u}, \mathbf{v}))$  with  $q_f(e(\mathbf{u}', \mathbf{v}'))$ 
20:     $\text{INTERSECTION}(e(\mathbf{u}, \mathbf{v}), e(\mathbf{u}', \mathbf{v}'), \mathcal{RG}_{f_1})$ 
21:  end for
22:  Mark  $e(\mathbf{u}, \mathbf{v})$  as processed
23: end for
24: return  $\mathcal{J}_f$ 

```

Computing intersection points. To check whether $q_f(e(\mathbf{u}, \mathbf{v}))$ has an intersection with $q_f(e(\mathbf{u}', \mathbf{v}'))$ at $q_f(\mathbf{x}) = q_f(\mathbf{y})$ we proceed as follows. We compute the projections of $e(\mathbf{u}, \mathbf{v})$ and $e(\mathbf{u}', \mathbf{v}')$ on the range of \mathbf{f} , i.e. \mathbb{R}^2 . If the line segments $\mathbf{f}(e(\mathbf{u}, \mathbf{v}))$ and $\mathbf{f}(e(\mathbf{u}', \mathbf{v}'))$ do not intersect, then for any $\mathbf{x} \in e(\mathbf{u}, \mathbf{v})$ and $\mathbf{y} \in e(\mathbf{u}', \mathbf{v}')$, we have $\mathbf{f}(\mathbf{x}) \neq \mathbf{f}(\mathbf{y})$, indicating that \mathbf{x} and \mathbf{y} do not lie on the same fiber, therefore, they cannot lie on the same fiber-component. On the other hand, if the line segments $\mathbf{f}(e(\mathbf{u}, \mathbf{v}))$ and $\mathbf{f}(e(\mathbf{u}', \mathbf{v}'))$ intersect, then there exist points $\mathbf{x} \in e(\mathbf{u}, \mathbf{v})$ and $\mathbf{y} \in e(\mathbf{u}', \mathbf{v}')$ such that \mathbf{x} and \mathbf{y} lie on the same fiber of \mathbf{f} . We then check if \mathbf{x} and \mathbf{y} also belong to the same fiber-component of \mathbf{f} .

We observe, if $q_{f_1}(\mathbf{x}) = q_{f_1}(\mathbf{y}) = p$ and $q_{\tilde{f}_2^p}(\mathbf{x}) = q_{\tilde{f}_2^p}(\mathbf{y})$ then \mathbf{x} and \mathbf{y} lie on the same fiber-component of \mathbf{f} , i.e. $q_f(\mathbf{x}) = q_f(\mathbf{y})$. In other words, if \mathbf{x} and \mathbf{y} are mapped to the same point in the first and corresponding second-dimensional Reeb graph of MDRG_f , then they lie on the same fiber-component. However, determining this requires exact computation of the intersection point of the line segments $\mathbf{f}(e(\mathbf{u}, \mathbf{v}))$ and $\mathbf{f}(e(\mathbf{u}', \mathbf{v}'))$, and checking if $q_{f_1}(\mathbf{x}) = q_{f_1}(\mathbf{y}) = p$ and $q_{\tilde{f}_2^p}(\mathbf{x}) = q_{\tilde{f}_2^p}(\mathbf{y})$ hold, overcoming floating-point errors, which are computationally challenging. Hence, we adopt the following strategy of analyzing the corresponding Reeb graphs in MDRG_f to decide if $q_f(\mathbf{x}) = q_f(\mathbf{y})$.

We note, if $\mathbf{f}(e(\mathbf{u}, \mathbf{v}))$ and $\mathbf{f}(e(\mathbf{u}', \mathbf{v}'))$ intersect, then there are three different possibilities, as illustrated in Figure 4(b)-(c). First, we consider q_{f_1} maps of $e(\mathbf{u}, \mathbf{v})$ and $e(\mathbf{u}', \mathbf{v}')$ in \mathcal{RG}_{f_1} . If $q_{f_1}(e(\mathbf{u}, \mathbf{v}))$ and $q_{f_1}(e(\mathbf{u}', \mathbf{v}'))$ have no intersection in \mathcal{RG}_{f_1} , then $q_{f_1}(\mathbf{x}) \neq q_{f_1}(\mathbf{y})$ for any

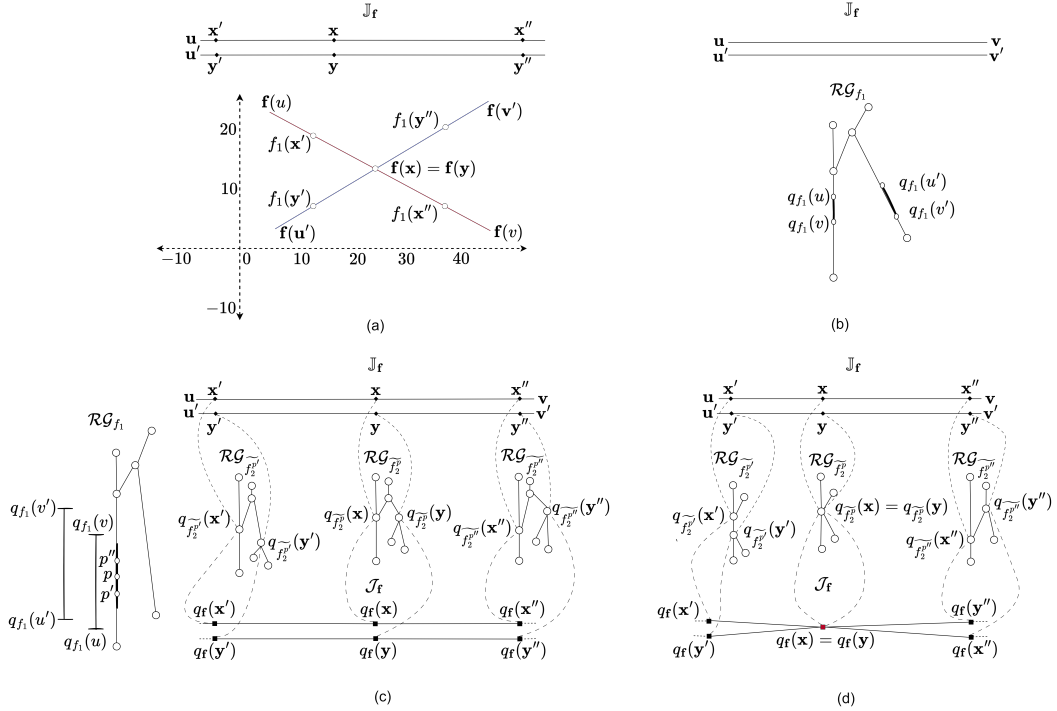
$\mathbf{x} \in e(\mathbf{u}, \mathbf{v})$ and $\mathbf{y} \in e(\mathbf{u}', \mathbf{v}')$ with $\mathbf{f}(\mathbf{x}) = \mathbf{f}(\mathbf{y})$ (see Figure 4(b)). Therefore, $q_{\mathbf{f}}(\mathbf{x}) \neq q_{\mathbf{f}}(\mathbf{y})$. However, if $q_{f_1}(e(\mathbf{u}, \mathbf{v}))$ and $q_{f_1}(e(\mathbf{u}', \mathbf{v}'))$ intersect, for $p \in q_{f_1}(e(\mathbf{u}, \mathbf{v})) \cap q_{f_1}(e(\mathbf{u}', \mathbf{v}'))$, let $q_{f_1}^{-1}(p)$ intersects $e(\mathbf{u}, \mathbf{v})$ and $e(\mathbf{u}', \mathbf{v}')$ at \mathbf{x} and \mathbf{y} , respectively. Therefore, $q_{f_1}(\mathbf{x}) = q_{f_1}(\mathbf{y}) = p$. In this case, there are two possibilities. If \mathbf{x} and \mathbf{y} belong to different contours of \tilde{f}_2^p (i.e. $q_{\tilde{f}_2^p}(\mathbf{x}) \neq q_{\tilde{f}_2^p}(\mathbf{y})$), then $q_{\mathbf{f}}(\mathbf{x}) \neq q_{\mathbf{f}}(\mathbf{y})$ (see Figure 4(c)). Otherwise, \mathbf{x} and \mathbf{y} are in the same fiber-component, i.e. $q_{\mathbf{f}}(\mathbf{x}) = q_{\mathbf{f}}(\mathbf{y})$, resulting in the intersection of $q_{\mathbf{f}}(e(\mathbf{u}, \mathbf{v}))$ and $q_{\mathbf{f}}(e(\mathbf{u}', \mathbf{v}'))$ (see Figure 4(d)). We note, this intersection point corresponds to the critical point of \tilde{f}_2^p where the second Morse condition is violated (as in Lemma 6-(C3)). In other words, this corresponds to the swapping of nodes or merge-split event in the second dimensional Reeb graphs, as observed in Figure 3(c). This event can be detected uniquely by analyzing the second dimensional Reeb graphs corresponding to points $p \in q_{f_1}(e(\mathbf{u}, \mathbf{v})) \cap q_{f_1}(e(\mathbf{u}', \mathbf{v}'))$.

More precisely, for $p \in q_{f_1}(e(\mathbf{u}, \mathbf{v})) \cap q_{f_1}(e(\mathbf{u}', \mathbf{v}'))$, let $q_{f_1}^{-1}(p)$ intersects $e(\mathbf{u}, \mathbf{v})$ and $e(\mathbf{u}', \mathbf{v}')$ at \mathbf{x} and \mathbf{y} , respectively. Then, if the nodes $q_{\tilde{f}_2^p}(\mathbf{x})$ and $q_{\tilde{f}_2^p}(\mathbf{y})$ are not connected by an arc in $\mathcal{RG}_{\tilde{f}_2^p}$ (case Figure 4(c)), $q_{\mathbf{f}}(e(\mathbf{u}, \mathbf{v}))$ and $q_{\mathbf{f}}(e(\mathbf{u}', \mathbf{v}'))$ do not intersect. Otherwise, if the nodes $q_{\tilde{f}_2^p}(\mathbf{x})$ and $q_{\tilde{f}_2^p}(\mathbf{y})$ are connected by an arc in $\mathcal{RG}_{\tilde{f}_2^p}$ (case Figure 4(d)), $q_{\mathbf{f}}(e(\mathbf{u}, \mathbf{v}))$ and $q_{\mathbf{f}}(e(\mathbf{u}', \mathbf{v}'))$ intersect. Moreover, at the point of intersection the nodes $q_{\tilde{f}_2^p}(\mathbf{x})$ and $q_{\tilde{f}_2^p}(\mathbf{y})$ coincide.

```

1: procedure INTERSECTION( $e(\mathbf{u}, \mathbf{v}), e(\mathbf{u}', \mathbf{v}'), \mathcal{RG}_{f_1}$ )
2:   % Check for the intersection of  $\mathbf{f}(e(\mathbf{u}, \mathbf{v}))$  and  $\mathbf{f}(e(\mathbf{u}', \mathbf{v}'))$ 
3:   if  $\mathbf{f}(e(\mathbf{u}, \mathbf{v}))$  and  $\mathbf{f}(e(\mathbf{u}', \mathbf{v}'))$  intersect then
4:     Compute:  $\mathbf{a} = \mathbf{f}(e(\mathbf{u}, \mathbf{v})) \cap \mathbf{f}(e(\mathbf{u}', \mathbf{v}'))$ 
5:     % Check for the intersection of  $q_{f_1}(e(\mathbf{u}, \mathbf{v}))$  and  $q_{f_1}(e(\mathbf{u}', \mathbf{v}'))$ 
6:     if  $q_{f_1}(e(\mathbf{u}, \mathbf{v}))$  and  $q_{f_1}(e(\mathbf{u}', \mathbf{v}'))$  intersect then
7:        $p \leftarrow q_{f_1}(e(\mathbf{u}, \mathbf{v})) \cap q_{f_1}(e(\mathbf{u}', \mathbf{v}'))$ 
8:        $\mathbf{x} \leftarrow q_{f_1}^{-1}(p) \cap e(\mathbf{u}, \mathbf{v})$ 
9:        $\mathbf{y} \leftarrow q_{f_1}^{-1}(p) \cap e(\mathbf{u}', \mathbf{v}')$ 
10:      % Construct the Augmented Reeb graph of  $\tilde{f}_2^p$ 
11:       $\mathcal{RG}_{\tilde{f}_2^p} = \text{CONSTRUCTAUGMENTEDREEBGRAPH}(q_{f_1}^{-1}(p), \tilde{f}_2^p)$ 
12:      if  $q_{\tilde{f}_2^p}(\mathbf{x})$  and  $q_{\tilde{f}_2^p}(\mathbf{y})$  are adjacent nodes of an arc in  $\mathcal{RG}_{\tilde{f}_2^p}$  then
13:        %  $q_{\mathbf{f}}(e(\mathbf{u}, \mathbf{v}))$  and  $q_{\mathbf{f}}(e(\mathbf{u}', \mathbf{v}'))$  have an intersection
14:        Add a vertex  $w$  in  $\mathcal{J}_{\mathbf{f}}$ 
15:        Subdivide  $e(q_{\mathbf{f}}(\mathbf{u}), q_{\mathbf{f}}(\mathbf{v}))$  into edges  $e(q_{\mathbf{f}}(\mathbf{u}), w)$  and  $e(w, q_{\mathbf{f}}(\mathbf{v}))$ 
16:        Subdivide  $e(q_{\mathbf{f}}(\mathbf{u}'), q_{\mathbf{f}}(\mathbf{v}'))$  into edges  $e(q_{\mathbf{f}}(\mathbf{u}'), w)$  and  $e(w, q_{\mathbf{f}}(\mathbf{v}'))$ 
17:        Set  $\bar{\mathbf{f}}(w) = \mathbf{a}$ 
18:         $\mathbf{x}_0 \leftarrow \mathbf{f}^{-1}(\mathbf{a}) \cap e(\mathbf{u}, \mathbf{v})$ 
19:         $\mathbf{y}_0 \leftarrow \mathbf{f}^{-1}(\mathbf{a}) \cap e(\mathbf{u}', \mathbf{v}')$ 
20:        Set  $q_{\mathbf{f}}(\mathbf{x}_0) = w$  and  $q_{\mathbf{f}}(\mathbf{y}_0) = w$ 
21:        Mark edges  $e(q_{\mathbf{f}}(\mathbf{u}), w), e(w, q_{\mathbf{f}}(\mathbf{v})), e(q_{\mathbf{f}}(\mathbf{u}'), w), e(w, q_{\mathbf{f}}(\mathbf{v}'))$  as processed
22:      else
23:         $q_{\mathbf{f}}(e(\mathbf{u}, \mathbf{v}))$  and  $q_{\mathbf{f}}(e(\mathbf{u}', \mathbf{v}'))$  do not intersect
24:      end if
25:    else
26:       $q_{\mathbf{f}}(e(\mathbf{u}, \mathbf{v}))$  and  $q_{\mathbf{f}}(e(\mathbf{u}', \mathbf{v}'))$  do not intersect
27:    end if
28:  else
29:     $q_{\mathbf{f}}(e(\mathbf{u}, \mathbf{v}))$  and  $q_{\mathbf{f}}(e(\mathbf{u}', \mathbf{v}'))$  do not intersect
30:  end if

```



32 **Figure 4 Self-intersection (double) points on the Jacobi structure:** For a bivariate
 33 field $\mathbf{f} = (f_1, f_2)$, (a) shows two edges $e(\mathbf{u}, \mathbf{v})$, $e(\mathbf{u}', \mathbf{v}')$ in different 1-manifold components of
 34 the Jacobi set $\mathbb{J}_{\mathbf{f}}$ with intersecting projections onto the range of \mathbf{f} . If $\exists \mathbf{x} \in e(\mathbf{u}, \mathbf{v}), \mathbf{y} \in e(\mathbf{u}', \mathbf{v}')$
 35 such that $\mathbf{f}(\mathbf{x}) = \mathbf{f}(\mathbf{y})$, then consider points $\mathbf{x}', \mathbf{x}'' \in e(\mathbf{u}, \mathbf{v})$ and $\mathbf{y}', \mathbf{y}'' \in e(\mathbf{u}', \mathbf{v}')$ with $f_1(\mathbf{x}') =$
 36 $f_1(\mathbf{y}') < f_1(\mathbf{x}) = f_1(\mathbf{y}) < f_1(\mathbf{x}'') = f_1(\mathbf{y}'')$. Three configurations of their projections onto the
 37 second-dimensional Reeb graphs of $\text{MDRG}_{\mathbf{f}}$ and the Jacobi structure $\mathcal{J}_{\mathbf{f}}$ are shown: (b) \mathbf{x} and \mathbf{y} lie
 38 in different contours of f_1 , (c) \mathbf{x} and \mathbf{y} belong to the same contour of f_1 but different contours of f_2 ,
 39 (d) \mathbf{x} and \mathbf{y} are in the same fiber-component of \mathbf{f} , and consequently $q_{\mathbf{f}}(\mathbf{x}) = q_{\mathbf{f}}(\mathbf{y})$ is a double point
 40 of $\mathcal{J}_{\mathbf{f}}$ (shown in red). The dotted lines illustrate the correspondence between points in the Jacobi
 41 set, Jacobi structure, and nodes in the Reeb graphs.

31: **end procedure**

Next, we discuss computing MDRG using the Jacobi structure.

5.3 Algorithm: Computing the MDRG

The computation of MDRG consists of the following four steps: (i) computing the Reeb graph \mathcal{RG}_{f_1} , (ii) determining the points of topological change along the arcs of \mathcal{RG}_{f_1} , (iii) augmenting the Reeb graph \mathcal{RG}_{f_1} based on the points of topological change, and (iv) selecting a representative point p from each subdivided arc and computing the augmented Reeb graph $\mathcal{RG}_{\tilde{f}_2^p}$. In the final step, the augmented Reeb graph signifies the inclusion of degree-2 nodes corresponding to the genus-change-only saddle critical points, as discussed in Section 3.2.2. We note, the nodes in these augmented Reeb graphs correspond to critical points of \tilde{f}_2^p , and consequently represent points in the Jacobi structure $\mathcal{J}_{\mathbf{f}}$ (see Section 5.2). Therefore, these nodes are crucial in capturing the topology of the Reeb space.

Algorithm 2 provides the pseudo-code for computing $\text{MDRG}_{\mathbf{f}}$. The first step for constructing $\text{MDRG}_{\mathbf{f}}$ involves the computation of the augmented Reeb graph \mathcal{RG}_{f_1} (line 3,

Algorithm 2) using an algorithm discussed in section 3.2.2. Next, we augment this Reeb graph further by determining the points of topological change which requires the computation of: (i) the minima of f_1 restricted to the Jacobi set \mathbb{J}_f , (ii) the maxima of f_1 restricted to \mathbb{J}_f , and (iii) double points of \mathcal{J}_f (see Lemma 6). The procedure COMPUTEJACOBI MINIMA provides the pseudo-code for determining the minima of f_1 on \mathbb{J}_f (line 4, Algorithm 2). A vertex $\mathbf{v} \in \mathbb{J}_f$ is identified as a minimum if $f_1(\mathbf{v})$ is less than the f_1 -values of its adjacent vertices in \mathbb{J}_f . The procedure for determining the maxima of f_1 in \mathbb{J}_f follows a similar approach (line 5, Algorithm 2). The DOUBLEPOINTS procedure computes points in \mathbb{M} mapped (by the quotient map q_f) to double-points in the Jacobi structure \mathcal{J}_f (line 6, Algorithm 2). The collective outcomes of these procedures constitute the points of topological change, denoted as P (line 7, Algorithm 2).

After determining P , the Reeb graph $\mathcal{R}\mathcal{G}_{f_1}$ is augmented by creating degree 2-nodes that correspond to the points in P . This is performed by the procedure AUGMENTREEBGRAPH (line 8, Algorithm 2). For each arc in the augmented Reeb graph, a representative p is selected by the procedure GETREPRESENTATIVEPOINT. Then, the augmented Reeb graph $\mathcal{R}\mathcal{G}_{f_2}^p$ is computed by the procedure CONSTRUCTAUGMENTEDREEBGRAPH (lines 12-14, Algorithm 2). The resulting augmented Reeb graphs $\mathcal{R}\mathcal{G}_{f_2}^p$ (with p as the representative point of an arc), along with the Reeb graph $\mathcal{R}\mathcal{G}_{f_1}$, collectively represent MDRG_f . These Reeb graphs are added to the set MDRG_f by the ADD procedure (lines 9, 14, Algorithm 2). The obtained MDRG is then utilized in the construction of the Reeb space.

■ **Algorithm 2** COMPUTEMDRG

Input: $\mathbb{M}, f, \mathbb{J}_f, \mathcal{J}_f$

Output: MDRG_f

```

1:  $\text{MDRG}_f = \emptyset$ 
2: % Augment First-Dimensional Reeb Graph with Additional Points of Topological Changes
3:  $\mathcal{R}\mathcal{G}_{f_1} = \text{CONSTRUCTAUGMENTEDREEBGRAPH}(\mathbb{M}, f_1)$ 
4:  $J_{min} = \text{COMPUTEJACOBI MINIMA}(\mathbb{J}_f, f_1, \mathcal{R}\mathcal{G}_{f_1})$ 
5:  $J_{max} = \text{COMPUTEJACOBI MAXIMA}(\mathbb{J}_f, f_1, \mathcal{R}\mathcal{G}_{f_1})$ 
6:  $DP = \text{DOUBLEPOINTS}(\mathcal{J}_f)$ 
7:  $P = J_{min} \cup J_{max} \cup DP$ 
8:  $\mathcal{R}\mathcal{G}_{f_1} = \text{AUGMENTREEBGRAPH}(\mathcal{R}\mathcal{G}_{f_1}, P)$ 
9:  $\text{MDRG}_f.\text{ADD}(\mathcal{R}\mathcal{G}_{f_1})$ 
10: % Computing Augmented Second-Dimensional Reeb Graphs
11: for arc  $\alpha \in \text{Arcs}(\mathcal{R}\mathcal{G}_{f_1})$  do
12:    $p = \text{GETREPRESENTATIVEPOINT}(\mathcal{R}\mathcal{G}_{f_1}, \alpha)$ 
13:    $\mathcal{R}\mathcal{G}_{f_2}^p = \text{CONSTRUCTAUGMENTEDREEBGRAPH}(q_{f_1}^{-1}(p), f_2)$ 
14:    $\text{MDRG}_f.\text{ADD}(\mathcal{R}\mathcal{G}_{f_2}^p)$ 
15: end for
16: return  $\text{MDRG}_f$ 

```

```

1: procedure COMPUTEJACOBI MINIMA( $\mathbb{J}_f, f_1, \mathcal{R}\mathcal{G}_{f_1}$ )
2:   Initialize:  $J_{min} = \emptyset$ 
3:   for  $\mathbf{v} \in \mathbb{J}_f$  do
4:     if  $q_{f_1}(\mathbf{v}) \notin V(\mathcal{R}\mathcal{G}_{f_1})$  then
5:        $N_{\mathbf{v}} = \mathbb{J}_f.\text{GetNeighbours}(\mathbf{v})$ 
6:        $\text{isMinimum} = \text{True}$ 
7:       for  $\mathbf{v}' \in N_{\mathbf{v}}$  do

```

```

8:         if  $f_1(\mathbf{v}') < f_1(\mathbf{v})$  then
9:             isMinimum = False
10:        end if
11:    end for
12:    if isMinimum = True then
13:        Add  $\mathbf{v}$  to  $J_{min}$ 
14:    end if
15: end if
16: end for
17: return  $J_{min}$ 
18: end procedure

1: procedure DOUBLEPOINTS( $\mathcal{J}_f$ )
2:   Initialize:  $DP = \emptyset$ 
3:   for  $v \in \mathcal{J}_f$  do
4:       if  $v$  is adjacent to four vertices then
5:           Get an arbitrary vertex  $\mathbf{v}$  from  $q_f^{-1}(v)$ 
6:           Add  $\mathbf{v}$  to  $DP$ 
7:       end if
8:   end for
9:   return  $DP$ 
10: end procedure

```

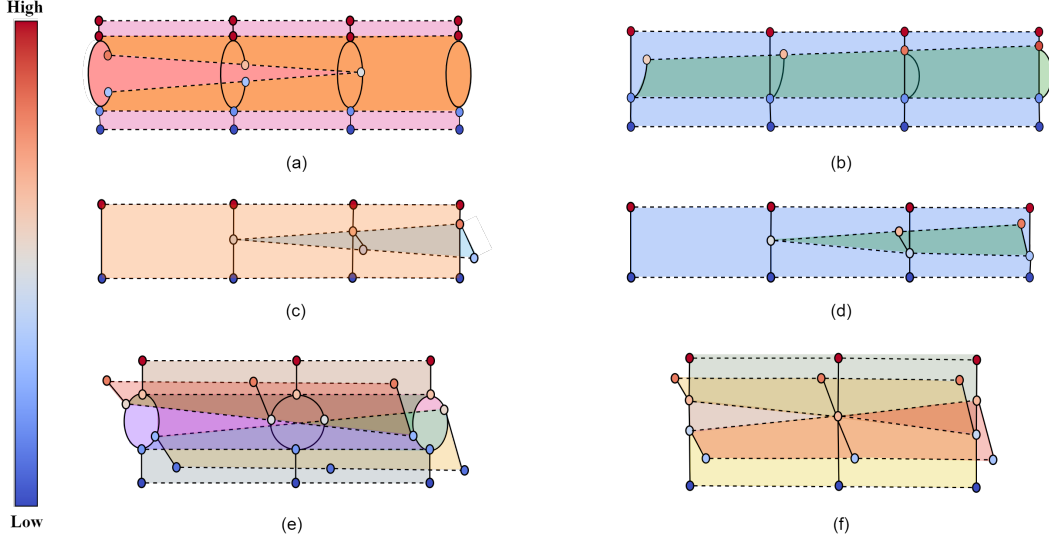
Finally, we discuss the main algorithm for approximating the Reeb space with a graph or net-like structure in the next subsection.

5.4 Algorithm: Computing the Reeb Space

In this subsection, we provide the algorithm for computing the net-like structure corresponding to the Reeb space. From Lemma 2, we note, the second-dimensional Reeb graphs in MDRG_f have an embedding in the Reeb space \mathcal{RS}_f . Therefore, to compute the Reeb space \mathcal{RS}_f we compute a topologically correct embedding of the second-dimensional Reeb graphs in MDRG_f by connecting them based on the computed Jacobi structure \mathcal{J}_f . First, we obtain a net-like structure or a skeleton corresponding to the Reeb space from which the sheets of the Reeb space can be visualized straightforwardly, as shown in Figure 5.

Algorithm 3 provides the pseudo-code for computing \mathcal{RS}_f . First, the Jacobi set \mathbb{J}_f is computed, as described in Section 5.2, by the procedure `COMPUTEJACOBISET` (line 1, Algorithm 3). Next, the Jacobi structure \mathcal{J}_f , which is the projection of the Jacobi set to the Reeb space, is computed using Algorithm 1 (line 2, Algorithm 3). Based on the Jacobi set and Jacobi structure, the MDRG_f is computed using Algorithm 2 (line 4, Algorithm 3). The first-dimensional augmented Reeb graph \mathcal{RG}_{f_1} is retrieved from MDRG_f by the procedure `GETFIRSTDIMENSIONALREEBGRAPH` (line 5, Algorithm 3). Then, for each arc α of \mathcal{RG}_{f_1} , a representative point p is obtained by the procedure `GETREPRESENTATIVEPOINT` (line 7, Algorithm 3). For each representative point p , the augmented Reeb graph $\mathcal{RG}_{\tilde{f}_2^p}$ is retrieved from MDRG_f , by the procedure `GETSECONDDIMENSIONALREEBGRAPH` (line 8, Algorithm 3). Then, $\mathcal{RG}_{\tilde{f}_2^p}$ is embedded in a net-like structure corresponding to \mathcal{RS}_f (line 9, Algorithm 3). The procedure `EMBEDREEBGRAPH` provides the pseudo-code for embedding an augmented Reeb graph $\mathcal{RG}_{\tilde{f}_2^p}$ in a net-like structure corresponding to \mathcal{RS}_f which is detailed next.

For an arc of $\mathcal{RG}_{\tilde{f}_2^p}$, the start and end nodes are extracted by the procedures `GETSTART-`



42 **Figure 5 Net-like structure corresponding to Reeb space:** (a)-(f) show the net-like
 43 structures corresponding to the Reeb spaces of the bivariate fields in Figures 1(b), 1(c), 2(b), 2(c),
 44 3(b), and 3(c), respectively. The sheets of the Reeb space are shown in different colors. The net-like
 45 structure consists of nodes and edges (represented by solid and dotted lines). The nodes and solid
 46 lines correspond to the nodes and edges in the second-dimensional Reeb graphs of the MDRG,
 47 respectively, and the dotted lines constitute the Jacobi structure. The coloring of the nodes in the
 48 net-like structure is based on the coloring of the corresponding nodes in the second-dimensional
 49 Reeb graphs.

NODE and GETENDNODE, respectively (lines 3 and 5, procedure EMBEDREEBGRAPH). For each arc β between two nodes p_1 and p_2 of $\mathcal{RG}_{\tilde{f}_2^p}$, an edge is introduced between the corresponding vertices in $\mathcal{J}_{\mathbf{f}}$, as follows. Since p is a point on an arc of the augmented Reeb graph \mathcal{RG}_{f_1} , the function \tilde{f}_2^p is essentially Morse (see Section 5.1 for more details). Therefore, the fiber-component of \mathbf{f} corresponding to p_1 contains exactly one critical point of \tilde{f}_2^p , denoted as \mathbf{x}_1 . This point is computed by the procedure GETJACOBISETPOINT (line 4, procedure EMBEDREEBGRAPH). As \mathbf{x}_1 is on the Jacobi set $\mathbb{J}_{\mathbf{f}}$, its projection $q_{\mathbf{f}}(\mathbf{x}_1)$ into $\mathcal{RS}_{\mathbf{f}}$ lies on $\mathcal{J}_{\mathbf{f}}$. Similarly, let \mathbf{x}_2 be the unique critical point of \tilde{f}_2^p corresponding to p_2 , and $q_{\mathbf{f}}(\mathbf{x}_2)$ denote its projection in $\mathcal{J}_{\mathbf{f}}$ (lines 6, procedure EMBEDREEBGRAPH). Then an edge between $q_{\mathbf{f}}(\mathbf{x}_1)$ and $q_{\mathbf{f}}(\mathbf{x}_2)$ is added to build the net-like structure corresponding to $\mathcal{RS}_{\mathbf{f}}$ (line 7, procedure EMBEDREEBGRAPH). Figure 5 shows the net-like structures corresponding to the Reeb spaces of the bivariate fields in Figures 1(b), 1(c), 2(b), 2(c), 3(b), and 3(c). The following lemma provides the proof of correctness for Algorithm 3.

► **Lemma 7. Proof of Correctness:** *Let $\mathbf{f} = (f_1, f_2)$ be a bivariate field defined on a compact 3-manifold without boundary. Then Algorithm 3 computes a net-like structure corresponding to the Reeb space of \mathbf{f} .*

Proof. From Proposition 4, we note, the $\text{MDRG}_{\mathbf{f}}$ is homeomorphic to $\mathcal{RS}_{\mathbf{f}}$. Specifically, the second-dimensional Reeb graphs of $\text{MDRG}_{\mathbf{f}}$ have an embedding in $\mathcal{RS}_{\mathbf{f}}$ (see Lemma 2). Therefore, by examining the variation in the topology of the second-dimensional Reeb graphs $\mathcal{RG}_{\tilde{f}_2^p}$, as p varies along arcs of \mathcal{RG}_{f_1} , the topology of the Reeb space is effectively captured. Let α be an arc in the Reeb graph \mathcal{RG}_{f_1} , which is augmented based on the points of topological change. Then the Reeb graphs in $\{\mathcal{RG}_{\tilde{f}_2^p} | p \in \alpha\}$ are topologically equivalent

(see Lemma 6). Therefore, for capturing the topology of these Reeb graphs, it is sufficient to choose a representative point p in α for computing the embedding of the Reeb graph $\mathcal{RG}_{f_2}^{\sim p}$ corresponding to $\mathcal{RS}_{\mathbf{f}}$.

However, it is essential to capture the topological variations in the second-dimensional Reeb graphs $\mathcal{RG}_{f_2}^{\sim p}$ as p varies across different arcs of \mathcal{RG}_{f_1} . We note, changes in the topology of $\mathcal{RG}_{f_2}^{\sim p}$ correspond to the critical points of f_2^p . These critical points are on the Jacobi set $\mathbb{J}_{\mathbf{f}}$. Since $\mathcal{J}_{\mathbf{f}}$ is the projection of $\mathbb{J}_{\mathbf{f}}$ to $\mathcal{RS}_{\mathbf{f}}$, the nodes of $\mathcal{RG}_{f_2}^{\sim p}$ embedded in $\mathcal{RS}_{\mathbf{f}}$ are located on $\mathcal{J}_{\mathbf{f}}$. Thus, $\mathcal{J}_{\mathbf{f}}$ tracks the topological changes in the second-dimensional Reeb graphs embedded in $\mathcal{RS}_{\mathbf{f}}$. Therefore, Algorithm 3 compute a topologically correct embedding of the second-dimensional Reeb graphs in $\text{MDRG}_{\mathbf{f}}$ corresponding to $\mathcal{RS}_{\mathbf{f}}$. ◀

■ **Algorithm 3** COMPUTEREEBSPACE

Input: \mathbb{M}, \mathbf{f}

Output: $\mathcal{RS}_{\mathbf{f}}$

```

1:  $\mathbb{J}_{\mathbf{f}} = \text{COMPUTEJACOBISET}(\mathbb{M}, \mathbf{f})$ 
2:  $\mathcal{J}_{\mathbf{f}} = \text{COMPUTEJACOBISTRUCTURE}(\mathbb{J}_{\mathbf{f}})$ 
3: Initialize:  $\mathcal{RS}_{\mathbf{f}} = \mathcal{J}_{\mathbf{f}}$ 
4:  $\text{MDRG}_{\mathbf{f}} = \text{COMPUTEMDRG}(\mathbb{M}, \mathbf{f}, \mathbb{J}_{\mathbf{f}}, \mathcal{J}_{\mathbf{f}})$ 
5:  $\mathcal{RG}_{f_1} = \text{GETFIRSTDIMENSIONALREEBGRAPH}(\text{MDRG}_{\mathbf{f}})$ 
6: for arc  $\alpha \in \text{Arcs}(\mathcal{RG}_{f_1})$  do
7:    $p = \text{GETREPRESENTATIVEPOINT}(\mathcal{RG}_{f_1}, \alpha)$ 
8:    $\mathcal{RG}_{f_2}^{\sim p} = \text{GETSECONDDIMENSIONALREEBGRAPH}(\text{MDRG}_{\mathbf{f}}, p)$ 
9:    $\text{EMBEDREEBGRAPH}(\mathcal{RG}_{f_2}^{\sim p}, \mathcal{RS}_{\mathbf{f}})$ 
10: end for
11: return  $\mathcal{RS}_{\mathbf{f}}$ 

```

```

1: procedure  $\text{EMBEDREEBGRAPH}(\mathcal{RG}_{f_2}^{\sim p}, \mathcal{RS}_{\mathbf{f}})$ 
2:   for  $\beta \in \text{Arcs}(\mathcal{RG}_{f_2}^{\sim p})$  do
3:      $p_1 = \text{GETSTARTNODE}(\beta)$ 
4:      $\mathbf{x}_1 = \text{GETJACOBISETPOINT}(p_1)$ 
5:      $p_2 = \text{GETENDNODE}(\beta)$ 
6:      $\mathbf{x}_2 = \text{GETJACOBISETPOINT}(p_2)$ 
7:     Add edge  $e(q_{\mathbf{f}}(\mathbf{x}_1), q_{\mathbf{f}}(\mathbf{x}_2))$  in  $\mathcal{RS}_{\mathbf{f}}$ 
8:   end for
9: end procedure

```

Next, we discuss the complexity of the proposed algorithms.

6 Complexity Analysis

In this section, we analyze the complexity of the proposed algorithm for computing the net-like structure corresponding to the Reeb space of a PL bivariate field $\mathbf{f} = (f_1, f_2) : \mathbb{M} \rightarrow \mathbb{R}^2$, defined on a triangulation \mathbb{M} of a 3-manifold. Let, the numbers of vertices, edges, triangles, and tetrahedra in \mathbb{M} be denoted as n_v , n_e , n_t , and n_T respectively, and the total number of simplices is given by $n = n_v + n_e + n_t + n_T$. Let j_v and j_e represent the number of vertices and edges of the Jacobi set $\mathbb{J}_{\mathbf{f}}$, respectively.

First, we provide the complexity analysis for computing the Jacobi structure \mathcal{J}_f (Algorithm 1). Next, we analyze the complexity of computing MDRG_f (Algorithm 2). Finally, we determine the complexity for computing the net-like structure corresponding to the Reeb space \mathcal{RS}_f (Algorithm 3).

6.1 Algorithm 1: Computing the Jacobi structure

The Jacobi structure \mathcal{J}_f is computed by individually processing each edge $e(\mathbf{u}, \mathbf{v})$ of the Jacobi set \mathbb{J}_f as follows. First, an edge between $q_f(\mathbf{u})$ and $q_f(\mathbf{v})$ is added in \mathcal{J}_f , which takes constant time (lines 4-16, Algorithm 1). Next, the augmented Reeb graph \mathcal{RG}_{f_1} is constructed, which takes $\mathcal{O}(n \log n)$ time (line 17, Algorithm 1). Note that this is the currently known lower bound on the complexity for computing the Reeb graph [6]. Finally, the intersection of the edge $e(q_f(\mathbf{u}), q_f(\mathbf{v}))$ is checked with the previously computed edges of \mathcal{J}_f (lines 18-21, Algorithm 1). To determine the time complexity of these lines, we assess the time complexity for the procedure INTERSECTION, which takes two edges $e(\mathbf{u}, \mathbf{v})$ and $e(\mathbf{u}', \mathbf{v}')$ of the Jacobi set as input, and determines the intersection of $e(q_f(\mathbf{u}), q_f(\mathbf{v}))$ and $e(q_f(\mathbf{u}'), q_f(\mathbf{v}'))$.

The first step in the procedure is determining the intersection of $\mathbf{f}(e(\mathbf{u}, \mathbf{v}))$ and $\mathbf{f}(e(\mathbf{u}', \mathbf{v}'))$ which takes constant time (line 3, procedure INTERSECTION). In the event of an intersection, the point of intersection a is computed (line 4, procedure INTERSECTION). Then, the projections of $e(u, v)$ and $e(u', v')$ on \mathcal{RG}_{f_1} (by the quotient map q_{f_1}) are examined for intersection, which also takes constant time (line 6, procedure INTERSECTION). If an intersection is found, then a point p within the intersecting region of \mathcal{RG}_{f_1} is selected (line 7, procedure INTERSECTION). Following this, the contour $q_{f_1}^{-1}(p)$ is computed, and the intersection of $q_{f_1}^{-1}(p)$ with the edges $e(\mathbf{u}, \mathbf{v})$ and $e(\mathbf{u}', \mathbf{v}')$ are determined, to obtain the points \mathbf{x} and \mathbf{y} , respectively (line 8-9, procedure INTERSECTION). The time complexity of computing $q_{f_1}^{-1}(p)$ and determining the intersections is bounded by $\mathcal{O}(n_T)$ [16]. The next step is the computation of the augmented Reeb graph $\mathcal{RG}_{\tilde{f}_2}$, which takes $\mathcal{O}(n' \log(n'))$ time, where n' is the number of simplices (vertices, edges, and triangles) of $q_{f_1}^{-1}(p)$ (line 11, procedure INTERSECTION). The overall complexity of lines 3-11 is $\mathcal{O}(n' \log(n') + n_T)$. Since $n_T \leq n$ and $n' \leq n$, this bound can be expressed as $\mathcal{O}(n \log(n) + n)$.

After this step, the adjacency of nodes $q_{\tilde{f}_2}(\mathbf{x})$ and $q_{\tilde{f}_2}(\mathbf{y})$ in $\mathcal{RG}_{\tilde{f}_2}$ is examined by checking the presence of $q_{\tilde{f}_2}(\mathbf{x})$ in the adjacency list of $q_{\tilde{f}_2}(\mathbf{y})$ (line 12, procedure INTERSECTION). The number of adjacent nodes of $q_{\tilde{f}_2}(\mathbf{x})$ is upper-bounded by the total number of nodes in $\mathcal{RG}_{\tilde{f}_2}$, which is in turn bounded above by n_v . Therefore, line 12 requires $\mathcal{O}(n_v)$ time. Finally, computing the intersection point of the projections of $e(\mathbf{u}, \mathbf{v})$ and $e(\mathbf{u}', \mathbf{v}')$ in \mathcal{RS}_f , and then subdividing the edges $e(q_f(\mathbf{u}), q_f(\mathbf{v}))$ and $e(q_f(\mathbf{u}'), q_f(\mathbf{v}'))$, take constant time (lines 13-20, procedure INTERSECTION). Hence, the total complexity of the procedure INTERSECTION is $\mathcal{O}(n \log(n) + n + n_v)$.

Since the for loop in line 18 of Algorithm 1 iterates through at most all the edges of \mathbb{J}_f , the time complexity for lines 18-21 is obtained as $\mathcal{O}(j_e(n \log(n) + n + n_v))$. Similarly, the for loop in line 2 iterates over all the edges of \mathbb{J}_f . Therefore, the time complexity of Algorithm 1 is $\mathcal{O}(j_e^2(n \log(n) + n + n_v))$. Since n and n_v are upper-bounded by $n \log(n)$, the bound can be simplified as $\mathcal{O}(nj_e^2 \log(n))$. In the next subsection, we analyze the time complexity for computing the MDRG.

6.2 Algorithm 2: Computing the MDRG

The computation of $\text{MDRG}_{\mathbf{f}}$ begins with the construction of the augmented Reeb graph \mathcal{RG}_{f_1} , which takes $\mathcal{O}(n \log(n))$ time (line 3, Algorithm 2). We note, this is the currently known lower bound on the complexity for computing the Reeb graph [6]. Line 4 invokes the procedure `COMPUTEJACOBI MINIMA` for computing the minima of f_1 restricted to $\mathbb{J}_{\mathbf{f}}$. Given that $\mathbb{J}_{\mathbf{f}}$ consists of PL 1-manifold components, each vertex of $\mathbb{J}_{\mathbf{f}}$ has at most two neighbours. Thus, determining whether a vertex of $\mathbb{J}_{\mathbf{f}}$ is a minimum of f_1 requires examining the f_1 -values of its neighbours, which takes constant time. Consequently, `COMPUTEJACOBI MINIMA` requires $\mathcal{O}(j_v)$ time. The time complexity for computing the maximum is similar (line 5, Algorithm 2). The procedure `DOUBLEPOINTS` identifies the double points of $\mathcal{J}_{\mathbf{f}}$ by examining the degree of every vertex. Therefore, this procedure takes time linear in the number of vertices of $\mathcal{J}_{\mathbf{f}}$. Since $\mathcal{J}_{\mathbf{f}}$ is the projection of $\mathbb{J}_{\mathbf{f}}$ onto the Reeb space, the time complexity of `DOUBLEPOINTS` is $\mathcal{O}(j_v)$ (line 6, Algorithm 2).

After this step, computing the union of J_{min} , J_{max} , and DP takes a time which linear in the cardinalities of these four sets. Let j_{min} and j_{max} represent the number of minima and maxima of f_1 restricted to $\mathbb{J}_{\mathbf{f}}$, respectively. Then cardinalities of J_{min} and J_{max} are upper-bounded by j_{min} and j_{max} , respectively. Further, the number double points of $\mathcal{J}_{\mathbf{f}}$ is upper-bounded by the number of vertices of $\mathbb{J}_{\mathbf{f}}$. Therefore, the time complexity of line 7 is $\mathcal{O}(j_{min} + j_{max} + j_v)$.

The next step is to augment the augmented Reeb graph \mathcal{RG}_{f_1} based on the additional points in P (line 8, Algorithm 2). For each point \mathbf{x} in P , the arc that contains $q_{f_1}(\mathbf{x})$ is split into two by introducing a node at $q_{f_1}(\mathbf{x})$. This operation takes constant time for each point in P . Thus, the complexity of line 8 is $\mathcal{O}(|P|)$, which is upper-bounded by $\mathcal{O}(j_{min} + j_{max} + j_v)$. The overall time taken by lines 1-9 is $\mathcal{O}(n \log(n) + 3j_v + 2(j_{min} + j_{max} + j_v))$. Next, we assess the complexity of lines 10-15.

For a representative point p of an arc α in \mathcal{RG}_{f_1} , computing the contour $q_{f_1}^{-1}(p)$ takes $\mathcal{O}(n_T)$ time [16]. The number of vertices and edges in $q_{f_1}^{-1}(p)$ are bounded by those of \mathbb{M} , leading to a $\mathcal{O}(n \log(n))$ complexity bound for the computation of $\mathcal{RG}_{\tilde{f}_2^p}$ (line 13, Algorithm 2). We note, the nodes in the augmented Reeb graph \mathcal{RG}_{f_1} constructed at line 8, correspond to either one of the following: (i) critical points of f_1 , (ii) critical points (minimum or maximum) of f_1 restricted to $\mathbb{J}_{\mathbf{f}}$, or (iii) double-points of $\mathcal{J}_{\mathbf{f}}$. The number of points in the first two categories is upper-bounded by $c_{f_1} + j_{min} + j_{max}$, and the number of double points is at most the number of vertices of $\mathbb{J}_{\mathbf{f}}$. Therefore, the number of nodes of \mathcal{RG}_{f_1} is at most $(c_{f_1} + j_{min} + j_{max} + j_v)$.

Given that f_1 is a generic PL Morse function, the up-degree (similarly down-degree) of a node of \mathcal{RG}_{f_1} can be at most 2 (see Section 3.2.2 for more details). Thus, the number of arcs of \mathcal{RG}_{f_1} is at most twice the number of nodes. Therefore, lines 11-15 take $\mathcal{O}(2(c_{f_1} + j_{min} + j_{max} + j_v)(n_T + n \log(n)))$ time. The total time complexity of Algorithm 2 is then given by $\mathcal{O}(n \log(n) + 3j_v + 2(j_{min} + j_{max} + j_v) + 2(c_{f_1} + j_{min} + j_{max} + j_v)(n_T + n \log(n)))$. Since n_T, j_v , and $(j_{min} + j_{max} + c_{f_1})$ are bounded above by n , the complexity bound can be expressed as $\mathcal{O}(n \log(n) + 7n + 4n(n + n \log(n))) \simeq \mathcal{O}(n^2 \log(n))$.

Next, we analyze the time complexity of the algorithm for computing the net-like structure corresponding to the Reeb space (Algorithm 3).

6.3 Algorithm 3: Computing the Reeb space

The computation of Reeb space starts with the construction of $\mathbb{J}_{\mathbf{f}}$, which takes $\mathcal{O}(n_e)$ time (line 1, Algorithm 3) [24]. Next, the computation of $\mathcal{J}_{\mathbf{f}}$ takes $\mathcal{O}(nj_e^2 \log(n))$ time (line 2,

Algorithm 3). Then, the MDRG is computed, which takes $\mathcal{O}(n^2 \log(n))$ (line 4, Algorithm 3). Next, we analyze the time complexity of lines 6-10 by determining the time complexity of the procedure `EMBEDREEBGRAPH`, which embeds the second-dimensional Reeb graphs of $\text{MDRG}_{\mathbf{f}}$.

For a representative point p of an arc in \mathcal{RG}_{f_1} , consider the augmented Reeb graph $\mathcal{RG}_{\tilde{f}_2^p}$. For an arc β of $\mathcal{RG}_{\tilde{f}_2^p}$, let p_1 and p_2 denote its start and end nodes. Then, the contour $q_{\tilde{f}_2^p}^{-1}(p_1)$ (similarly $q_{\tilde{f}_2^p}^{-1}(p_2)$) contains at least one critical point of \tilde{f}_2^p . From Lemma 6, it follows that \tilde{f}_2^p is a Morse function. Therefore, $q_{\tilde{f}_2^p}^{-1}(p_1)$ contains exactly one critical point, say \mathbf{x}_1 , as the presence of more than one would violate the second Morse condition. Since \mathbf{x}_1 is a critical point of f_2 restricted to a level set of f_1 , it lies on the Jacobi set. To project \mathbf{x}_1 onto $\mathcal{RS}_{\mathbf{f}}$ (by the quotient map $q_{\mathbf{f}}$), we need to determine the edge of $\mathbb{J}_{\mathbf{f}}$ containing \mathbf{x}_1 . This requires examining all edges of $\mathbb{J}_{\mathbf{f}}$, and takes $\mathcal{O}(j_e)$ time. Thus line 4 (and similarly lines 6) of the procedure `EMBEDREEBGRAPH` take $\mathcal{O}(j_e)$ time. After this step, the addition of an edge in $\mathcal{J}_{\mathbf{f}}$ corresponding to the projection of β takes constant time (line 7, procedure `EMBEDREEBGRAPH`).

The complexity of the for loop in line 2 of the procedure `EMBEDREEBGRAPH` is bounded by the number of arcs of $\mathcal{RG}_{\tilde{f}_2^p}$. Since \tilde{f}_2^p is Morse, the number of arcs in $\mathcal{RG}_{\tilde{f}_2^p}$ is at most twice the number of nodes (as discussed in Section 6.2). Let $c_{\tilde{f}_2^p}$ denote the number of critical points of \tilde{f}_2^p . Then, the time complexity of the procedure `EMBEDREEBGRAPH` is $\mathcal{O}(2c_{\tilde{f}_2^p}(2j_e)) \simeq \mathcal{O}(4c_{\tilde{f}_2^p}j_e)$.

The for loop in line 2 of Algorithm 3 takes time linear in the number of arcs of \mathcal{RG}_{f_1} . However, the total number of critical points $c_{\tilde{f}_2^p}$, over the representative points of all the arcs, is at most the number of vertices in the mesh. In other words, we have $\sum_{\alpha \in \mathcal{RG}_{f_1}} c_{\tilde{f}_2^p} \leq n_v$, where p is the representative point of the arc α . Therefore, lines 6-10 of Algorithm 3 take $\mathcal{O}(4n_v j_e)$ time. The total time complexity of Algorithm 3 is then $\mathcal{O}(n_e + n j_e^2 \log(n) + n^2 \log(n) + 2(c_{f_1} + j_{\min} + j_{\max} + j_v) + 4n_v j_e)$. Since the terms n_e , j_v , c_{f_1} , and $(j_{\min} + j_{\max})$ are upper-bounded by n , the complexity bound can be simplified as $\mathcal{O}(n j_e^2 \log(n) + n^2 \log(n))$.

7 Conclusion

In this paper, we present the first algorithm for computing a net-like structure embedded in the Reeb space of a PL bivariate field without relying on the range-quantization. First, we prove a homeomorphism between the MDRG of a bivariate field and its Reeb space. Following that, we introduce a novel algorithm for computing the Jacobi structure. Then, an algorithm for computing the MDRG based on the Jacobi set and Jacobi structure is provided. Finally, we devise an algorithm for computing the net-like structure corresponding to the Reeb space utilizing the MDRG and the Jacobi structure. We provide the proof of correctness of our algorithm. A thorough analysis of the time complexity has also been presented for each of the algorithms.

However, the theory and algorithms introduced in the current paper are specifically designed for bivariate fields. Future work will focus on extending them for general PL multi-fields. It is important to highlight that the net-like structure of the Reeb space for a bivariate field encapsulates the joint topological features of both fields in a concise 1-dimensional structure. Therefore, this work harbors potential for applications across diverse computational domains, requiring exploration in future studies.

References

- 1 Tripti Agarwal, Amit Chattopadhyay, and Vijay Natarajan. Topological feature search in time-varying multifield data. In Ingrid Hotz, Talha Bin Masood, Filip Sadlo, and Julien Tierny, editors, *Topological Methods in Data Analysis and Visualization VI*, pages 197–217, Cham, 2021. Springer International Publishing.
- 2 H. Carr and D. Duke. Joint contour nets. *IEEE Transactions on Visualization and Computer Graphics*, 20(8):1100–1113, Aug 2014. doi:10.1109/TVCG.2013.269.
- 3 Hamish Carr, Zhao Geng, Julien Tierny, Amit Chattopadhyay, and Aaron Knoll. Fiber surfaces: Generalizing isosurfaces to bivariate data. *Computer Graphics Forum*, 34(3):241–250, 2015. doi:10.1111/cgf.12636.
- 4 A. Chattopadhyay, H. Carr, D. Duke, Z. Geng, and O. Saeki. Multivariate topology simplification. *Computational Geometry: Theory and Application*, 58:1–24, 2016.
- 5 Yi-Jen Chiang and Xiang Lu. Progressive simplification of tetrahedral meshes preserving all isosurface topologies. *Computer Graphics Forum*, 22(3):493–504, 2003. arXiv:https://onlinelibrary.wiley.com/doi/pdf/10.1111/1467-8659.00697, doi:10.1111/1467-8659.00697.
- 6 Tamal Krishna Dey and Yusu Wang. *Computational Topology for Data Analysis*. Cambridge University Press, 2022. doi:10.1017/9781009099950.
- 7 Harish Doraiswamy and Vijay Natarajan. Computing reeb graphs as a union of contour trees. *IEEE transactions on visualization and computer graphics*, 19, 04 2012. doi:10.1109/TVCG.2012.115.
- 8 David Duke, Hamish Carr, Aaron Knoll, Nicolas Schunck, Hai Ah Nam, and Andrzej Staszczak. Visualizing nuclear scission through a multifield extension of topological analysis. *IEEE Transactions on Visualization and Computer Graphics*, 18(12):2033–2040, 2012. doi:10.1109/TVCG.2012.287.
- 9 Herbert Edelsbrunner and John Harer. Jacobi Sets of Multiple Morse Functions. In *Foundations of Computational Mathematics, Minneapolis, 2002*, pages 37–57, 2004. Cambridge Univ. Press, 2004.
- 10 Herbert Edelsbrunner and John Harer. *Computational Topology - an Introduction*. American Mathematical Society, 2010.
- 11 Herbert Edelsbrunner, John Harer, Ajith Mascarenhas, Valerio Pascucci, and Jack Snoeyink. Time-varying reeb graphs for continuous space–time data. *Computational Geometry*, 41(3):149–166, 2008. URL: https://www.sciencedirect.com/science/article/pii/S09257772107001071, doi:10.1016/j.comgeo.2007.11.001.
- 12 Herbert Edelsbrunner, John Harer, and Amit K. Patel. Reeb spaces of piecewise linear mappings. In *Proceedings of the Twenty-Fourth Annual Symposium on Computational Geometry*, SCG '08, page 242–250, New York, NY, USA, 2008. Association for Computing Machinery. doi:10.1145/1377676.1377720.
- 13 Martin Golubitsky and Victor W. Guillemin. Stable mappings and their singularities. 1973. URL: https://api.semanticscholar.org/CorpusID:119015259.
- 14 William Harvey, Yusu Wang, and Rephael Wenger. A randomized $O(m \log m)$ time algorithm for computing reeb graphs of arbitrary simplicial complexes. In *Proceedings of the Twenty-Sixth Annual Symposium on Computational Geometry*, SoCG '10, page 267–276, New York, NY, USA, 2010. Association for Computing Machinery. doi:10.1145/1810959.1811005.
- 15 Daniel Klötzl, Tim Krake, Youjia Zhou, Ingrid Hotz, Bei Wang, and Daniel Weiskopf. Local bilinear computation of jacobi sets. *The Visual Computer*, 38:1–14, 06 2022. doi:10.1007/s00371-022-02557-4.
- 16 Y. Livnat, Han-Wei Shen, and C.R. Johnson. A near optimal isosurface extraction algorithm using the span space. *IEEE Transactions on Visualization and Computer Graphics*, 2(1):73–84, 1996. doi:10.1109/2945.489388.
- 17 Salman Parsa. A deterministic $O(m \log m)$ time algorithm for the reeb graph. *Discrete & Computational Geometry*, 49, 06 2012. doi:10.1145/2261250.2261289.

- 18 Yashwanth Ramamurthi, Tripti Agarwal, and Amit Chattopadhyay. A topological similarity measure between multi-resolution reeb spaces. *IEEE Transactions on Visualization and Computer Graphics*, pages 1–1, 2021. doi:10.1109/TVCG.2021.3087273.
- 19 Yashwanth Ramamurthi and Amit Chattopadhyay. A topological distance between multi-fields based on multi-dimensional persistence diagrams. *IEEE Transactions on Visualization and Computer Graphics*, pages 1–14, 2023. doi:10.1109/TVCG.2023.3314763.
- 20 Osamu Saeki. *Topology of Singular Fibers of Differentiable Maps*. Springer, 2004.
- 21 Osamu Saeki, Shigeo Takahashi, Daisuke Sakurai, Hsiang-Yun Wu, Keisuke Kikuchi, Hamish Carr, David Duke, and Takahiro Yamamoto. Visualizing multivariate data using singularity theory. In Masato Wakayama, Robert S. Anderssen, Jin Cheng, Yasuhide Fukumoto, Robert McKibbin, Konrad Polthier, Tsuyoshi Takagi, and Kim-Chuan Toh, editors, *The Impact of Applications on Mathematics*, pages 51–65, Tokyo, 2014. Springer Japan.
- 22 Mohit Sharma and Vijay Natarajan. Jacobi set driven search for flexible fiber surface extraction. In *2022 Topological Data Analysis and Visualization (TopoInVis)*, pages 49–58, 2022. doi:10.1109/TopoInVis57755.2022.00012.
- 23 Gurjeet Singh, Facundo Memoli, and Gunnar Carlsson. Topological Methods for the Analysis of High Dimensional Data Sets and 3D Object Recognition. In M. Botsch, R. Pajarola, B. Chen, and M. Zwicker, editors, *Eurographics Symposium on Point-Based Graphics*. The Eurographics Association, 2007. doi:10.2312/SPBG/SPBG07/091-100.
- 24 Julien Tierny and Hamish Carr. Jacobi fiber surfaces for bivariate reeb space computation. *IEEE Transactions on Visualization and Computer Graphics*, 23(1):960–969, 2017. doi:10.1109/TVCG.2016.2599017.